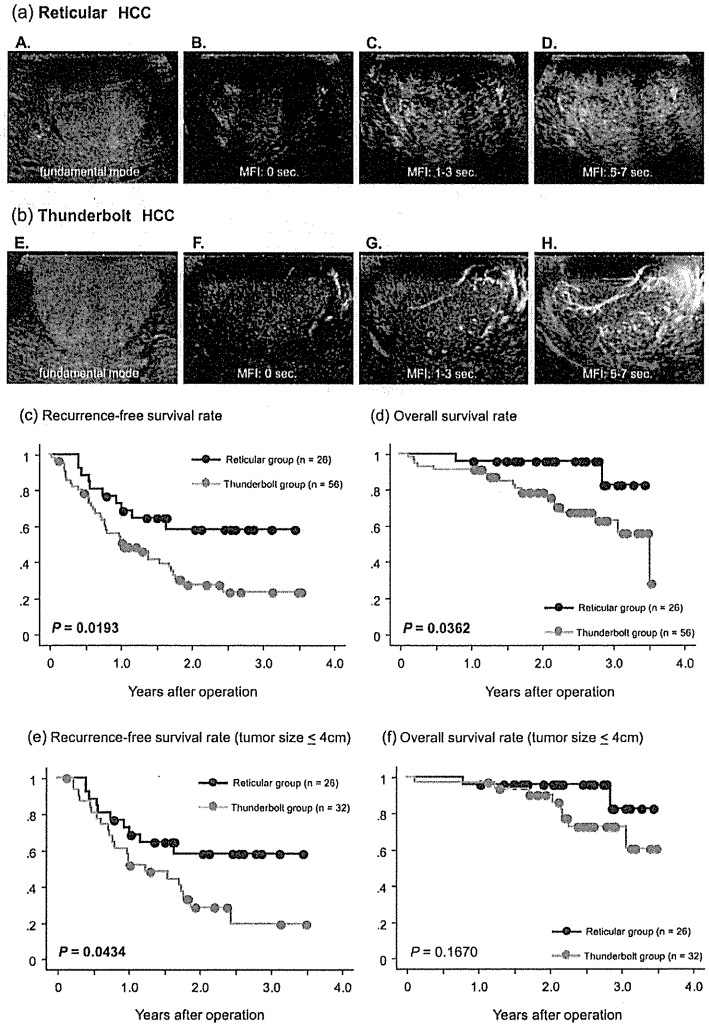

Fig. 1. Classification of CEIOUS MFI patterns with HCC. Using the MFI data, the HCC vasculatures were classified into two characteristic types; (a) reticular HCC and (b) thunderbolt HCC. While reticular HCC was gradually enhanced to the entire tumor with thin and ramified vessels (B-D), thunderbolt HCC was enhanced in a part of tumor with thick and linear vessels (F-H). The fundamental mode of ultrasonography is shown (A, E). (c) Recurrence-free survival and (d) overall survival of patients with HCC according to the MFI patterns. A log-rank test demonstrated statistically significant differences in recurrence-free and overall survival rates ($P = 0.0193$ and $P = 0.0362$, respectively). (e) Recurrence-free survival and (f) overall survival curves of the patients with HCC ≤4 cm. A log-rank test demonstrated statistically significant differences in the recurrence-free survival rates ($P = 0.0434$).

Table 2. Clinicopathological Findings in Patients with HCC in Relation to MFI Patterns of CEIOUS

Clinicopathological Factor	MFI Pattern: Reticular HCC (n = 26)	MFI Pattern: Thunderbolt HCC (n = 56)	P
Age, years, mean ± SD	69.5 ± 8.0	65.8 ± 9.3	0.0868
Sex, no., male:female	20:6	42:14	0.8503
Viral infection, no., HBV:HCV:non-B/C	4:12:10	9:34:13	0.3416
Background liver pathology, no.			0.5341
Normal	3	3	
Chronic hepatitis or liver fibrosis	11	22	
Liver cirrhosis	12	31	
Child-Pugh classification, no.			0.7676
A	25	53	
B	1	3	
Albumin, mg/dL, mean ± SD	4.1 ± 0.4	4.0 ± 0.5	0.6408
Total bilirubin, mg/dL, mean ± SD	0.82 ± 0.40	0.94 ± 0.40	0.2060
PT%, mean ± SD	83.3 ± 6.2	81.7 ± 8.6	0.3899
AFP, no., ≥20 ng/mL			0.0003
Yes	5	35	
No	21	21	
PIVKA-II, no., ≥40 mAU/mL			0.6779
Yes	15	35	
No	11	21	
Tumor size, cm, mean ± SD	2.6 ± 0.9	4.9 ± 3.9	0.0048
Tumor number, no., solitary:multiple	17:9	32:24	0.4788
Histological differentiation, no.			0.0004
Well/moderate	22	24	
Poor	4	32	
Tumor morphology, no.			0.1981
Simple nodular type	13	24	
Simple nodular type with extranodular growth	9	13	
Confluent multinodular type	4	19	
Tumor growth type, no.			0.0215
Expansive growth	26	46	
Infiltrative growth	0	10	
Portal vein invasion, no.			<0.0001
Negative	25	17	
Microinvasion	1	24	
Macroinvasion	0	15	
Hepatic vein invasion, no.			0.1680
Negative	24	45	
Positive	2	11	
Bile duct invasion, no.			0.1623
Negative	26	52	
Positive	0	4	
Capsule formation, no.			0.7087
Negative	8	15	
Positive	18	41	
Cancerous infiltration of the capsule, no.			0.7632
Negative	13	26	
Positive	13	30	
Formation of fibrous septum within the tumor, no.			0.3594
Negative	8	12	
Positive	18	44	
TNM stage, no., I/II:III/IV	20:6	13:43	<0.0001

Abbreviations: HBV, hepatitis B virus; HCV, hepatitis C virus; PIVKA-II, protein induced by vitamin K absence or antagosists II.

detected preoperatively using other imaging modalities (Supporting Table 1). In the 82 cases, 26 were classified as reticular HCC, and the remaining 56 cases were classified as thunderbolt HCC (Fig. 1a,b). The clinicopathological significance of the MFI patterns was then evaluated. Univariate analysis revealed that thunderbolt HCC correlated significantly

Table 3. Clinicopathological Findings in Patients with HCC in Relation to MFI Patterns of CEIOUS (Tumor Size Limited to ≤4 cm)

Clinicopathological Factor	MFI Pattern: Reticular HCC (n = 26)	MFI Pattern: Thunderbolt HCC (n = 32)	P
Age, years, mean ± SD	69.5 ± 8.0	67.5 ± 7.9	0.3548
Sex, no., male:female	20:6	22:10	0.4886
Viral infection, no., HBV:HCV:non-B/C	4:12:10	3:21:8	0.3291
Background liver pathology, no.			0.2809
Normal	3	1	
Chronic hepatitis or liver fibrosis	11	12	
Liver cirrhosis	12	19	
Child-Pugh classification, no.			0.4086
A	25	29	
B	1	3	
Albumin, mg/dL, mean ± SD	4.1 ± 0.4	4.1 ± 0.5	0.8200
Total bilirubin, mg/dL, mean ± SD	0.82 ± 0.40	0.97 ± 0.42	0.1853
PT%, mean ± SD	83.3 ± 6.2	81.0 ± 8.4	0.2383
AFP, no., ≥20 ng/mL			0.0009
Yes	5	20	
No	21	12	
PIVKA-II, no., ≥40 mAU/mL			0.5592
Yes	15	16	
No	11	16	
Tumor size, cm, mean ± SD	2.6 ± 0.9	2.9 ± 0.8	0.3004
Tumor number, no., solitary:multiple	17:9	21:11	0.9847
Histological differentiation, no.			0.0014
Well/moderate	22	14	
Poor	4	18	
Tumor morphology, no.			0.5256
Simple nodular type	13	19	
Simple nodular type with extranodular growth	9	5	
Confluent multinodular type	4	8	
Tumor growth type, no.			0.2217
Expansive growth	26	28	
Infiltrative growth	0	4	
Portal vein invasion, no.			<0.0001
Negative	25	12	
Microinvasion	1	13	
Macroinvasion	0	7	
Hepatic vein invasion, no.			0.2245
Negative	24	26	
Positive	2	6	
Bile duct invasion, no.			0.3632
Negative	26	31	
Positive	0	1	
Capsule formation, no.			0.6249
Negative	8	8	
Positive	18	24	
Cancerous infiltration of the capsule, no.			0.8128
Negative	13	17	
Positive	13	15	
Formation of fibrous septum within the tumor, no.			0.4417
Negative	8	7	
Positive	18	25	
TNM stage, no., I/II:III/IV	20:6	10:22	0.0005

Abbreviations: HBV, hepatitis B virus; HCV, hepatitis C virus; PIVKA-II, protein induced by vitamin K absence or antagosists II.

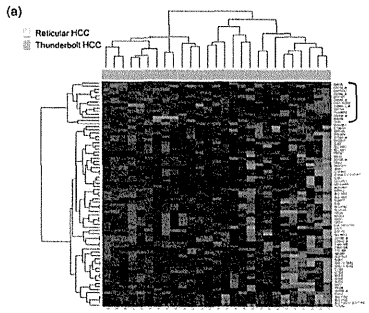

(b)

Probe set	Gene symbol	Gene title	*P value*	FC
218350_s_at	GMNN	geminin, DNA re-replication inhibitor	0.00326	2.15
230795_at	---	---	0.00392	2.10
238807_at	GAPDHL7	glyceraldehyde-3-phosphate dehydrogenase-like 7	0.00001	2.24
222366_at	---	---	0.00786	2.11
211721_s_at	ZNF551	zinc finger protein 551	0.00786	2.09
238040_at	---	---	0.00786	2.06
210387_at	HIST1H2BG	histone cluster 1, H2bg	0.00062	2.16
239069_s_at	---	---	0.00222	2.23
235405_at	GSTA4	glutathione S-transferase alpha 4	0.00665	2.04
1553145_at	FLJ39653	hypothetical FLJ39653	0.00470	2.18
235456_at	---	---	0.00392	2.13
203304_at	BAMBI	BMP and activin membrane-bound inhibitor homolog	0.00270	2.74
210665_at	TFPI	tissue factor pathway inhibitor	0.00926	2.51
210613_s_at	SYNGR1	synaptogyrin 1	0.00097	2.63

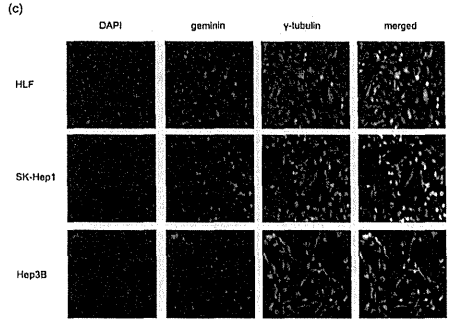

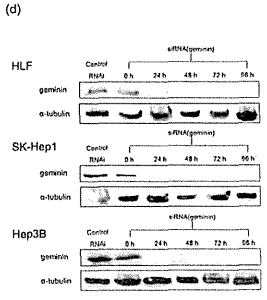

Fig. 2. Molecular and biological analysis in relation to the MFI patterns of HCC. (a) Gene expression profiling and MFI patterns. The hierarchical clustering of the gene expression (FC >2 and $P < 0.01$) in reticular HCC (blue bars) and thunderbolt HCC (orange bars). Dendrograms show the classification determined by the hierarchical clustering analysis. The red and green areas indicate relative overexpression and underexpression, respectively. (b) The differentially expressed genes in thunderbolt HCC by ranking of FC and *P* value (FC > 2, $P < 0.01$). The profiling identified geminin as one of the dominant molecules significantly overexpressed in cancer tissue of thunderbolt HCC. (c) Immunocytochemical analysis of geminin in human HCC cell lines (original magnification ×200). The predominant expression was recognized in the nucleus. DAPI, 4',6-diamidino-2-phenylindeole. (d) The silencing effects of the geminin gene. Western blot analysis confirmed that the geminin expression was markedly suppressed by the specific siRNA, compared with control siRNA (siNegative) in HLF, SK-Hep1, and Hep3B human HCC cells. (e) Growth curve analysis up after siRNA transfection. The silenced HLF, SK-Hep1 and Hep3B cells showed a significant reduction in cell proliferation. *$P <$ 0.01 versus control. The results are presented as the mean ± SD from triplicate experiments. (f) Cell cycle analyses. The percentage of <2N DNA content cells was increased in all cell lines after transfection of geminin siRNA.

with high levels of alpha-fetoprotein (AFP) ($P = 0.0003$), tumor size ($P = 0.0048$), histological dedifferentiation ($P = 0.0004$), infiltrative growth type ($P = 0.0215$), portal vein invasion ($P < 0.0001$), and tumor-node-metastasis (TNM) stage ($P < 0.0001$) (Table 2).

The recurrence-free survival and overall survival rates were then compared between the two groups. The thunderbolt HCC group demonstrated a significantly poorer prognosis than the reticular HCC group for both recurrence-free survival ($P = 0.0193$) and overall survival ($P = 0.0362$) (Fig. 1c,d). In order to exclude the bias of tumor size, we analyzed the significance of MFI patterns by limiting the tumor size to ≤4 cm in diameter. As a result, patients with thunderbolt HCC demonstrated a poorer recurrence-free survival than those with reticular HCC (Fig. 1e,f). As shown in Table 3, thunderbolt HCC also correlated significantly with high levels of AFP, histological dedifferentiation, portal vein invasion, and TNM stage, even if the tumor size was ≤4 cm.

Genome-wide Gene Expression Analysis Correlated to the MFI Patterns of Human HCC. Gene expression was analyzed in 27 samples of HCC,

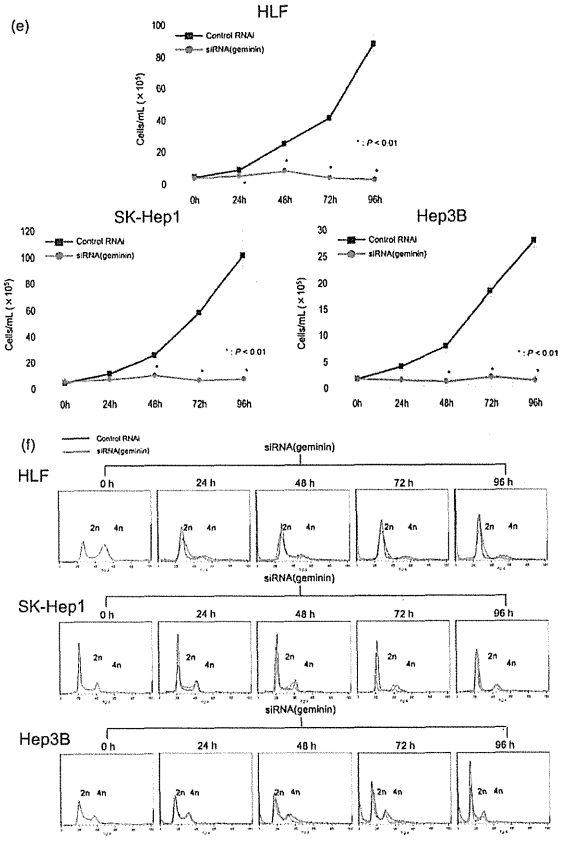

Fig. 2. (Continued)

including 11 reticular HCCs and 16 thunderbolt HCCs. The gene expression changes in 72 probe sets were evaluated by microarray analysis in 27 HCCs (FC >2, $P < 0.01$). As shown in Fig. 2a, the hierarchical clustering clearly divided the samples, and 14 genes were up-regulated in thunderbolt HCC. As displayed in Fig. 2b, in order of the FC and *P* values, a rereplication inhibitor geminin was significantly overexpressed in thunderbolt HCCs.

Significance of Geminin Expression in Human HCC Cells. The expression of the geminin protein was then analyzed in human HCC cell lines. The protein expression was recognized by western blotting in all of eight cell lines examined. Among them, we selected the three cell lines according to the expression level of geminin (HLF, high; SK-Hep1, moderate; Hep3B, low). Immunocytochemical analysis in these cell lines showed the potent expression of geminin protein, mainly in the nucleus (Fig. 2c). Next, the effects of the specific siRNAs against geminin were assessed in the HCC cell lines (HLF, SK-Hep1, and Hep3B). Western blot analysis certified that the expression of geminin was markedly silenced by the specific siRNA, but not by the control siRNA (Fig. 2d).

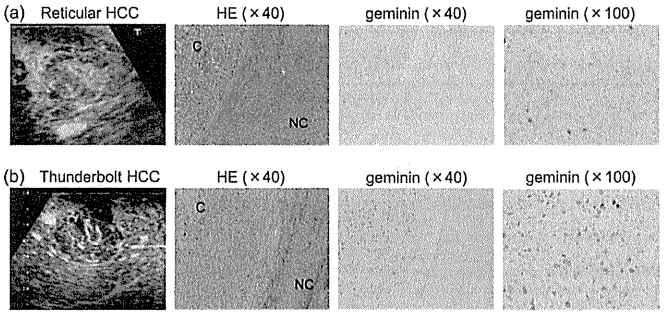

(c)

	Reticular HCC (n = 26)	Thunderbolt HCC (n = 26)	*P* value
geminin positive cells rate(%)	3.1 ± 0.6 (0.2 - 13.6)	9.3 ± 0.9 (0.6 - 32.1)	**< 0.0001**
geminin			**< 0.0001**
(-) (< 5%)	22	15	
(+) (≥ 5%, < 10%)	3	19	
(++) (≥ 10%)	1	22	

Fig. 3. Immunohistochemical analysis of expression of geminin protein in cancer tissues (C) and noncancerous tissues (NC) of human HCC. Compared with the cancer tissue of reticular HCC (a), the expression of geminin protein was increased in the cancer tissue of thunderbolt HCC (b). In noncancerous tissue of HCC, the expression of geminin was not detected. (c) Mean percentages of geminin-positive cells in cancer tissues (upper) and the case numbers of each type HCC (lower).

As shown in the cell growth assays of HCC (Fig. 2e), geminin siRNA significantly depressed cellular proliferation 96 hours after transfection, compared with cells treated with control siRNA ($P < 0.01$). In addition, cell cycle analysis demonstrated the accumulation of <2N DNA content in all of the cell lines after transfection of geminin siRNA (Fig. 2f). These results suggest that geminin has an essential role in the cell cycling of human HCC.

MFI Pattern of HCC Tumors and the Expression of Geminin Protein. Immunohistochemical validation of geminin protein was then performed using 82 tissue samples of HCC. As a shown in Fig. 3, the geminin protein stained mainly in the nucleus was clearly detected in cancer cells of HCC, but not in noncancerous liver tissue. The frequency of geminin-positive cancer cells was 9.3% in thunderbolt HCCs, but only 3.1% in reticular HCCs, indicating the statistical significance between the two types ($P < 0.0001$). The statistical significance was also observed even if the tumor size was limited (Supporting Table 3). The geminin expression and MFI patterns were not associated with cholangiocellular differentiation as well as progenitor cell markers (Supporting Fig. 1). According to the multivariate analysis for the MFI patterns of HCC using logistic regression mode, the expression of geminin protein ($P = 0.0180$), tumor size ($P = 0.0222$), and portal vein invasion ($P = 0.0174$) were statistically independent factors of MFI thunderbolt HCC (Table 4).

Postoperative Outcomes of HCC Patients and the Expression of Geminin Protein. The clinicopathological significance of geminin expression was then evaluated in the 82 patients enrolled in this study (Table 5). The univariate analysis for overall survival

Table 4. Multivariate Analysis for Independent Predictors of MFI Patterns of HCC

Clinicopathological Factor	HR (95% CI)	*P*
AFP ≥20 ng/mL	3.276 (0.464-23.145)	0.2342
Tumor size, cm	3.704 (1.206-11.378)	0.0222
Histological differentiation		
Well/moderate:poor	6.082 (0.669-55.320)	0.1090
Tumor growth type		
Eg:Ig	NA	0.9813
Portal vein invasion		
Negative:Positive	43.968 (1.945-993.935)	0.0174
TNM stage (I/II:III/IV)	4.341 (0.287-65.582)	0.2892
Geminin	1.289 (1.044-1.590)	0.0180

CI, confidence interval; Eg, expansive growth; HR, hazard ratio; Ig, infiltrative growth; NA, not applicable.

Table 5. Univariate and Multivariate Analysis of Overall Survival

	Univariate Analysis		Multivariate Analysis	
Clinicopathological Factor	HR (95% CI)	*P*	HR (95% CI)	*P*
Age, years	1.026 (0.972-1.083)	0.3745		
Sex, male versus female	1.333 (0.441-4.034)	0.6107		
Viral infection		0.8216		
HBV	1.814 (0.408-8.076)			
HCV	0.456 (0.168-1.297)			
Non-B/C	1.703 (0.556-5.124)			
Background liver pathology		0.5585		
Normal	0.635 (0.145-2.780)			
Chronic hepatitis or liver fibrosis	0.949 (0.371-2.430)			
Liver cirrhosis	1.218 (0.488-3.040)			
Child-Pugh classification, A versus B	2.246 (0.516-9.784)	0.2810		
Albumin	0.355 (0.150-0.842)	0.0187	0.619 (0.213-1.804)	0.3797
PT%	0.969 (0.921-1.019)	0.2205		
Total bilirubin	0.894 (0.293-2.728)	0.8446		
AFP, ng/mL, ≥20 versus <20	4.562 (1.511-13.771)	0.0071	1.780 (0.484-6.555)	0.3856
PIVKA-II, mAU/mL, ≥40 versus < 40	1.856 (0.668-5.160)	0.2357		
Tumor size, cm	1.035 (0.978-1.157)	0.1510		
Tumor number, solitary versus multiple	2.930 (1.151-7.462)	0.0242	2.254 (0.607-8.371)	0.2247
Histological differentiation, well/moderate versus poor	3.327 (1.276-8.677)	0.0140	1.137 (0.303-4.259)	0.8492
Tumor morphology, SN/SNEG versus CM	2.178 (0.895-5.299)	0.0863		
Tumor growth type, Eg versus Ig	3.636 (1.374-9.624)	0.0093	2.588 (0.664-10.088)	0.1706
Portal vein invasion	2.183 (0.869-5.481)	0.0965		
Hepatic vein invasion	4.140 (1.621-10.575)	0.0030	5.039 (1.441-17.627)	0.0113
Bile duct invasion	2.103 (0.273-16.217)	0.4757		
Capsule formation	1.571 (0.168-3.996)	0.3427		
Cancerous infiltration of the capsule	1.455 (0.584-3.624)	0.4205		
Formation of fibrous septum within the tumor	1.251 (0.415-3.778)	0.6907		
TNM stage, I/II versus III/IV	3.392 (1.129-10.186)	0.0295	1.332 (0.255-6.965)	0.7339
Geminin	1.120 (1.053-1.192)	0.0003	1.098 (1.017-1.185)	0.0170

CI, confidence interval; CM, confluent multinodular type; Eg, expansive growth; HBV, hepatitis B virus; HCV, hepatitis C virus; HR, hazard ratio; Ig, infiltrative growth; PIVKA-II, protein induced by vitamin K absence or antagonists II; SN, simple nodular type; SNEG, simple nodular type with extranodular growth.

of HCC revealed that the expression of geminin protein ($P = 0.0003$), serum level of albumin ($P = 0.0187$) and AFP ($P = 0.0071$), tumor number ($P = 0.0242$), histological dedifferentiation ($P = 0.0140$), infiltrative growth type ($P = 0.0093$), hepatic vein invasion ($P = 0.0030$), and TNM stage ($P = 0.0074$) were significantly for overall survival of HCC. The multivariate analysis revealed that the expression of geminin protein ($P = 0.0170$) and hepatic vein invasion ($P = 0.0113$) were statistically independent factors of overall survival.

Discussion

Tumor angiogenesis is one of the special features of HCC progression, and the detection of abnormal vasculature in a focal liver lesion aids in the identification of HCC.[14,15,18-21] Previous studies have reported that contrast-enhanced ultrasonography using microbubble-based contrast agents is useful for visualizing the vasculature of HCC.[22,23] In particular, the difference in vasculature of HCC and surrounding liver could be evaluated in detail using MFI with contrast agents.[23,34] Although some studies reported that CEIOUS was useful for detection of focal HCC lesions during hepatic resection, the significance of CEIOUS findings of MFI has not yet been clarified.[35,36]

In this study, we investigated the MFI with Sonazoid CEIOUS in hepatic resection for HCC. The MFI pattern was classified as reticular HCC and thunderbolt HCC, and as shown in Table 2 and Fig. 1c,d, thunderbolt HCC was significantly associated with the advanced progression and poor prognosis. We also revealed that the thunderbolt pattern was useful to predict the microinvasion into portal veins, which were undetectable by preoperative imaging modalities (Table 2). A subgroup analysis limiting the tumor size to ≤4 cm also demonstrated advanced progression and poorer prognosis in thunderbolt HCC compared with reticular HCC (Fig. 1e,f and Table 3). Additionally, we found the clinicopathological differences between each MFI pattern even when the tumor size was limited to <3 cm or <5 cm (Supporting Table 2).

To clarify the molecular and biological features associated with the MFI patterns, the gene expression profiling was further evaluated in human HCC

samples (Fig. 2a). The gene expression analysis identified geminin as one of the dominant molecules significantly overexpressed in thunderbolt HCC tissue (Fig. 2b). Geminin is known as a DNA rereplication inhibitor that is expressed in the G2, S, and M phases but not in the G0 and G1 phases.[37,38] DNA replication begins with assembly of prereplication complexes (preRCs) at multiple sites throughout the genome as cells exit metaphase.[39] preRCs are then assembled into preinitiation complexes that are subsequently activated by protein kinases to begin DNA synthesis (S phase). Once S phase begins, further assembly of preRCs is prevented by phosphorylation, ubiquitination, and degradation of preRC proteins ORC1, CDC6, and CDT1, and by geminin, a specific protein inhibitor of CDT1 activity unique to metazoan.[40,41]

Previous studies have reported that geminin is specifically expressed in proliferating cells, including lymphocytes, crypt epithelial cells, and sperm cells, but not in nonproliferating epithelial cells, including normal neurocytes, muscle cells, and hepatocytes.[42,43] As for malignant neoplasms, the overexpression of geminin was reported in advanced human cancers such as breast, lung, renal, and colorectal carcinomas.[41,44-48] According to our additional analysis, Ki67 expression was significantly associated with geminin expression ($P = 0.0112$), supporting the proliferative role of geminin in HCC (Supporting Fig. 2). Indeed, *in vitro* knockdown of geminin significantly suppressed the cell proliferation of human HCC cell lines (Fig. 2d-f).

Our immunohistochemical analysis on clinical samples clarified that the frequency of geminin-positive cancer cells correlated significantly with thunderbolt HCCs (Fig. 3 and Supporting Table 3). In addition, the clinical significance of geminin was noted in the overall survival (Table 5). Quaglia et al.[49] reported that the expression level of geminin was increased from regenerative and dysplastic nodules to HCC nodules, indicating its potential association with hepatocarcinogenesis. The molecular and biological role of geminin in HCC progression should be studied further.

In conclusion, the intraoperative MFI patterns were independent predictors of HCC progression, resulting in poor prognosis of the patients. Such vascular patterns were distinctly identified by gene expression profiling, such as geminin, which might play roles in HCC cell proliferation. Application of CEIOUS might be useful in determining the postoperative treatment of HCC. Additional studies should clarify the clinical impacts of CEIOUS MFI patterns.

Reference

1. Parkin DM, Bray F, Ferlay J, Pisani P. Estimating the world cancer burden: Globocan 2000. Int J Cancer 2001;94:153-156.
2. Hashem B, El-Serag. Hepatocellular carcinoma. N Engl J Med 2011; 365:1118-1127.
3. Cha CH, Saif MW, Yamane BH, Weber SM. Hepatocellular carcinoma: current management. Curr Probl Surg 2010;47:10-67.
4. Arii S, Yamaoka Y, Futagawa S, Inoue K, Kobayashi K, Kojiro M, et al. Results of surgical and nonsurgical treatment for small-sized hepatocellular carcinomas: a retrospective and nationwide survey in Japan. The Liver Cancer Study Group of Japan. HEPATOLOGY 2000;32: 1224-1229.
5. Hanish SI, Knechtle SJ. Liver transplantation for the treatment of hepatocellular carcinoma. Oncology (Williston Park) 2011;25:752-757.
6. Kruskal JB, Kane RA. Intraoperative US of the liver: techniques and clinical applications. Radiographics 2006;26:1067-1084.
7. Postema M, Gilja OH. Contrast-enhanced and targeted ultrasound. World J Gastroenterol 2011;17:28-41.
8. Sontum PC. Physicochemical characteristics of Sonazoid, a new contrast agent for ultrasound imaging. Ultrasound Med Biol 2008;34: 824-833.
9. Watanabe R, Matsumura M, Chen CJ, Kaneda Y, Ishihara M, Fujimaki M. Gray-scale liver enhancement with Sonazoid (NC100100), a novel ultrasound contrast agent; detection of hepatic tumors in a rabbit model. Biol Pharm Bull 2003;26:1272-1277.
10. Mandai M, Koda M, Matono T, Nagahara T, Sugihara T, Ueki M, et al. Assessment of hepatocellular carcinoma by contrast-enhanced ultrasound with perfluorobutane microbubbles: comparison with dynamic CT. Br J Radiol 2011;84:499-507.
11. Goto E, Masuzaki R, Tateishi R, Kondo Y, Imamura J, Goto T, et al. Value of post-vascular phase (Kupffer imaging) by contrast-enhanced ultrasonography using Sonazoid in the detection of hepatocellular carcinoma. J Gastroenterol 2012;47:477-485.
12. Sugimoto K, Shiraishi J, Moriyasu F, Saito K, Doi K. Improved detection of hepatic metastases with contrast-enhanced low mechanical-index pulse inversion ultrasonography during the liver-specific phase of sonazoid: observer performance study with JAFROC analysis. Acad Radiol 2009;16:798-809.
13. Mitsunori Y, Tanaka S, Nakamura N, Ban D, Irie T, Noguchi N, et al. Contrast-enhanced intraoperative ultrasound for hepatocellular carcinoma: high sensitivity of diagnosis and therapeutic impact. J Hepatobiliary Pancreat Sci 2012; doi:10.1007/s00534-012-0507-9.
14. Carmeliet P, Jain RK. Angiogenesis in cancer and other diseases. Nature 2000;407:249-257.
15. Carmeliet P, Jain RK. Molecular mechanisms and clinical applications of angiogenesis. Nature 2011;473:298-307.
16. Eberhard A, Kahlert S, Goede V, Hemmerlein B, Plate KH, Augustin HG. Heterogeneity of angiogenesis and blood vessel maturation in human tumors: implications for antiangiogenic tumor therapies. Cancer Res 2000;60:1388-1393.
17. Baish JW, Jain RK. Fractals and cancer. Cancer Res 2000;60: 3683-3688.
18. Tanaka S, Arii S. Current status and perspective of antiangiogenic therapy for cancer: hepatocellular carcinoma. Int J Clin Oncol 2006;11: 82-89.
19. Llovet JM, Ricci S, Mazzaferro V, Hilgard P, Gane E, Blanc JF, et al; SHARP Investigators Study Group. Sorafenib in advanced hepatocellular carcinoma. N Engl J Med 2008;359:378-390.
20. Tanaka S, Sugimachi K, Yamashita Yi Y, Ohga T, Shirabe K, Shimada M, Wands JR, et al. Tie2 vascular endothelial receptor expression and function in hepatocellular carcinoma. HEPATOLOGY 2002;35: 861-867.
21. Toyoda H, Fukuda Y, Hayakawa T, Kumada T, Nakano S. Changes in blood supply in small hepatocellular carcinoma: correlation of angiographic images and immunohistochemical findings. J Hepatol 1997;27: 654-660.

22. Ogawa S, Kumada T, Toyoda H, Ichikawa H, Kawachi T, Otobe K, et al. Evaluation of pathological features of hepatocellular carcinoma by contrast-enhanced ultrasonography: comparison with pathology on resected specimen. Eur J Radiol 2006;59:74-81.
23. Sugimoto K, Moriyasu F, Kamiyama N, Metoki R, Yamada M, Imai Y, et al. Analysis of morphological vascular changes of hepatocellular carcinoma by microflow imaging using contrast-enhanced sonography. Hepatol Res 2008;38:790-799.
24. Asayama Y, Yoshimitsu K, Nishihara Y, Irie H, Aishima S, Taketomi A, et al. Arterial blood supply of hepatocellular carcinoma and histologic grading: radiologic-pathologic correlation. AJR Am J Roentgenol 2008;190:28-34.
25. Tarhan NC, Hatipoğlu T, Ercan E, Bener M, Keleş G, Bayaran C, et al. Correlation of dynamic multidetector CT findings with pathological grades of hepatocellular carcinoma. Diagn Interv Radiol 2011;17:328-333.
26. Quackenbush J. Microarray analysis and tumor classification. N Engl J Med 2006;354:2463-2472.
27. Hoshida Y, Villanueva A, Kobayashi M, Peix J, Chiang DY, Camargo A, et al. Gene expression in fixed tissues and outcome in hepatocellular carcinoma. N Engl J Med 2008;359:1995-2004.
28. Aihara A, Tanaka S, Yasen M, Matsumura S, Mitsunori Y, Murakata A, et al. The selective Aurora B kinase inhibitor AZD1152 as a novel treatment for hepatocellular carcinoma. J Hepatol 2010;52:63-71.
29. Murakata A, Tanaka S, Mogushi K, Yasen M, Noguchi N, Irie T, et al. Gene expression signature of the gross morphology in hepatocellular carcinoma. Ann Surg 2011;253:94-100.
30. Yoshitake K, Tanaka S, Mogushi K, Aihara A, Murakata A, Matsumura S, et al. Importin-α1 as a novel prognostic target for hepatocellular carcinoma. Ann Surg Oncol 2011;18:2093-2103.
31. Tanaka S, Arii S, Yasen M, Mogushi K, Su NT, Zhao C, et al. Aurora kinase B is a predictive factor for the aggressive recurrence of hepatocellular carcinoma after curative hepatectomy. Br J Surg 2008;95:611-619.
32. Liver Cancer Study Group of Japan. The general rules for the clinical and pathological study of primary liver cancer. 3rd ed. Tokyo; 2010.
33. Tanaka S, Pero SC, Taguchi K, Shimada M, Mori M, Krag DN, et al. Specific peptide ligand for Grb7 signal transduction protein and pancreatic cancer metastasis. J Natl Cancer Inst 2006;98:491-498.
34. Sugimoto K, Shiraishi J, Moriyasu F, Ichimura S, Metoki R, Doi K. Analysis of intrahepatic vascular morphological changes of chronic liver disease for assessment of liver fibrosis stages by micro-flow imaging with contrast-enhanced ultrasound: preliminary experience. Eur Radiol 2010;20:2749-2757.
35. Nanashima A, Tobinaga S, Abo T, Kunizaki M, Takeshita H, Hidaka S, et al. Usefulness of sonazoid-ultrasonography during hepatectomy in patients with liver tumors: a preliminary study. J Surg Oncol 2011; 103:152-157.
36. Arita J, Takahashi M, Hata S, Shindoh J, Beck Y, Sugawara Y, et al. Usefulness of contrast-enhanced intraoperative ultrasound using sonazoid in patients with hepatocellular carcinoma. Ann Surg 2011;254: 992-999.
37. Xouri G, Dimaki M, Bastiaens PI, Lygerou Z. Cdt1 interactions in the licensing process: a model for dynamic spatiotemporal control of licensing. Cell Cycle 2007;6:1549-1552.
38. Karamitros D, Kotantaki P, Lygerou Z, Veiga-Fernandes H, Pachnis V, Kioussis D, et al. Life without geminin. Cell Cycle 2010;9:3181-3185.
39. Noguchi K, Vassilev A, Ghosh S, Yates JL, DePamphilis ML. The BAH domain facilitates the ability of human Orc1 protein to activate replication origins in vivo. EMBO J 2006;25:5372-5382.
40. DePamphilis ML, Blow JJ, Ghosh S, Saha T, Noguchi K, Vassilev A. Regulating the licensing of DNA replication origins in metazoa. Curr Opin Cell Biol 2006;18:231-239.
41. Blow JJ, Gillespie PJ. Replication licensing and cancer—a fatal entanglement? Nat Rev Cancer 2008;8:799-806.
42. Wohlschlegel JA, Kutok JL, Weng AP, Dutta A. Expression of geminin as a marker of cell proliferation in normal tissues and malignancies. Am J Pathol 2002;161:267-273.
43. Eward KL, Obermann EC, Shreeram S, Loddo M, Fanshawe T, Williams C, et al. DNA replication licensing in somatic and germ cells. J Cell Sci 2004;117:5875-5886.
44. Gonzalez MA, Tachibana KE, Chin SF, Callagy G, Madine MA, Vowler SL, et al. Geminin predicts adverse clinical outcome in breast cancer by reflecting cell-cycle progression. J Pathol 2004;204:121-130.
45. Dudderidge TJ, Stoeber K, Loddo M, Atkinson G, Fanshawe T, Griffiths DF, et al. Mcm2, Geminin, and Ki67 define proliferative state and are prognostic markers in renal cell carcinoma. Clin Cancer Res 2005;11:2510-2517.
46. Nishihara K, Shomori K, Tamura T, Fujioka S, Ogawa T, Ito H. Immunohistochemical expression of geminin in colorectal cancer: implication of prognostic significance. Oncol Rep 2009;21:1189-1195.
47. Haruki T, Shomori K, Hamamoto Y, Taniguchi Y, Nakamura H, Ito H. Geminin expression in small lung adenocarcinomas: implication of prognostic significance. Lung Cancer 2011;71:356-362.
48. Zhu W, Depamphilis ML. Selective killing of cancer cells by suppression of geminin activity. Cancer Res 2009;69:4870-4877.
49. Quaglia A, McStay M, Stoeber K, Loddo M, Caplin M, Fanshawe T, et al. Novel markers of cell kinetics to evaluate progression from cirrhosis to hepatocellular carcinoma. Liver Int 2006;26:424-432.

Ann Surg Oncol (2013) 20:305–317
DOI 10.1245/s10434-012-2395-2

Annals of
SURGICAL ONCOLOGY
OFFICIAL JOURNAL OF THE SOCIETY OF SURGICAL ONCOLOGY

ORIGINAL ARTICLE – HEPATOBILIARY TUMORS

Upregulation of Protein Tyrosine Phosphatase Type IVA Member 3 (PTP4A3/PRL-3) is Associated with Tumor Differentiation and a Poor Prognosis in Human Hepatocellular Carcinoma

Abudureheman Mayinuer, MD[1], Mahmut Yasen, MD, PhD[1,2], Kaoru Mogushi, PhD[3], Gulanbar Obulhasim, MD, PhD[1,2], Maimaiti Xieraili, MD[1], Arihiro Aihara, MD, PhD[1], Shinji Tanaka, MD, PhD[1], Hiroshi Mizushima, PhD[3], Hiroshi Tanaka, PhD[3], and Shigeki Arii, MD, PhD, FACS[1]

[1]Department of Hepato-Biliary-Pancreatic Surgery, Tokyo Medical and Dental University, Tokyo, Japan; [2]Department of Surgery, Xinjiang Uyghur Tumor Hospital of Xinjiang Medical University, Xinjiang, China; [3]Department of Computational Biology and Bioinformatics, Tokyo Medical and Dental University, Tokyo, Japan

ABSTRACT

Background. Protein tyrosine phosphatase type IVA member 3 (PTP4A3/PRL-3), a metastasis-associated phosphatase, plays multiple roles in cancer metastasis. We investigated PTP4A3/PRL-3 expression and its correlation with the clinicopathological features and prognosis in hepatocellular carcinoma (HCC).

Methods. Gene expression profiles of PTP4A3/PRL-3 were obtained in poorly differentiated HCC tissues. The results were validated independently by TaqMan gene expression assays and immunohistochemical analysis.

Results. According to the microarray profiles, PTP4A3/PRL-3 was upregulated in patients with poorly differentiated disease compared to patients with well-differentiated disease with hepatic backgrounds associated with hepatitis B or C. Validation analysis showed that the PTP4A3/PRL-3 mRNA and protein levels were significantly associated with poor differentiation ($P < 0.0001$), high serum α-fetoprotein ($P < 0.01$), high serum protein induced by vitamin K absence/antagonist-II (PIVKA-II), and hepatic vascular invasion ($P < 0.05$). The expression of PTP4A3/PRL-3 protein was also correlated with advanced cancer stages ($P < 0.01$); this resulted in a significantly poorer prognosis in both overall ($P = 0.0024$) and recurrence-free survival ($P = 0.0227$). According Cox regression univariate analysis, the positive expression of PTP4A3/PRL-3 was a poor risk prognostic factor (OS, $P = 0.0031$; recurrence-free survival, $P = 0.0245$). Cox regression multivariate analysis indicated that high PTP4A3/PRL-3 expression was an independent, unfavorable prognostic factor for overall survival (hazard ratio 0.542; $P = 0.048$).

Conclusions. PTP4A3/PRL-3 might be closely associated with HCC progression, invasion, and metastasis. Its high expression had a negative impact on the prognosis of HCC patients. This strongly suggests that PTP4A3/PRL-3 should be considered as a prognostic factor. Further analysis should be pursued to evaluate it as a novel prognostic target.

Hepatocellular carcinoma (HCC) is one of the most common malignant tumors worldwide.[1] Although surgical resection is a potentially curative treatment for HCC, and despite improved diagnosis and advances in surgical and nonsurgical therapies, the clinical outcome of HCC remains poor.[2,3] It is therefore crucial to understand the molecular mechanisms of this highly aggressive cancer, and finding molecular markers that can predict the tumor prognosis is important for developing new therapies.

Protein tyrosine phosphatase type IVA, member 3 (PTP4A3), is also known as phosphatase of regenerating liver-3 (PRL-3). It is a member of the PRL subgroup of protein tyrosine phosphatases, which are a large family of regulatory enzymes that function actively with protein tyrosine kinases in signaling pathways and participate in many

Electronic supplementary material The online version of this article (doi:10.1245/s10434-012-2395-2) contains supplementary material, which is available to authorized users.

First Received: 21 November 2011;
Published Online: 13 October 2012

S. Arii, MD, PhD, FACS
e-mail: ars.msrg@tmd.ac.jp

fundamental physiological processes.[4–6] Accumulating evidence suggests that PRL phosphatases, especially PRL-3, have been involved in the proliferation, growth regulation, increased cell motility, metastasis, and invasion in different types of cancers.[7–9] It has been reported that PRL-3 was specifically overexpressed in liver metastases derived from colorectal cancer as well as invasive breast cancer, ovarian cancer, gastric cancer, esophageal squamous cell carcinoma, and squamous cell carcinoma of the cervix.[10–13] Furthermore, PRL-3 was demonstrated to be a useful indicator for tumor recurrence and patient outcome in several human cancers.[14–21] In HCC, PRL-3 was found to be overexpressed, and it was closely associated with tumor invasion and angiogenesis.[22] However, up to now, the expression of PTP4A3/PRL-3 and its clinicopathological and prognostic significance in HCC have not been determined.

DNA microarray technology has enabled us to analyze the genome-wide profile of gene expression specific to malignant tumors. Such studies have the potential to lead to the development of a novel, molecular-targeted therapy for HCC.[23] In the present study, PTP4A3/PRL-3 was obtained in poorly differentiated HCC tissues by examining the genome-wide expression profile of HCC generated by cDNA microarray. The results of training analyses, which were validated independently by TaqMan gene expression assays and immunohistochemically, and their clinicopathological significance, including the prognosis and recurrence of HCC, were investigated.

MATERIALS AND METHODS

Patients and Preparation of Tissue Samples

We enrolled 256 patients undergoing partial hepatectomy for the first time of primary HCC between 2001 and 2010 at the Tokyo Medical and Dental University Hospital. The hepatitis virus status of these patients was as follows: 59 patients were positive for hepatitis B virus (HBV) surface antigen, 144 were positive for hepatitis C virus (HCV) antibody, and 53 were negative for both. In addition, 90 patients were pathologically diagnosed as having well-differentiated HCC, 91 moderately differentiated, and 75 poorly differentiated. In this study, we selected patients who were virus infected and whose HCC was either well or poorly differentiated, according to pathological diagnosis. A total of 142 primary liver tumor specimens (virus-negative patients and moderate-differentiation HCC tissues were excluded) and 10 normal liver specimens (which came from metastatic liver cancer patients whose origin tumor was diagnosed as colorectal cancer) were collected during surgery, snap frozen in liquid nitrogen, and stored at −80 °C. A portion of the tissue sample was fixed in 10 % formaldehyde solution and embedded in paraffin for histopathological analysis. Written informed consent was obtained from these patients, and the institutional review board approved the study. The patients were followed up with assays of their serum level of α-fetoprotein (AFP) and protein induced by vitamin K absence or antagonists II every month, and by ultrasonography, computed tomography (CT), and magnetic resonance imaging every 3 months.

Microarray Gene Expression

Gene expression analysis was performed on the 42 primary HCC patients whose samples were used as training sets, and samples from the remaining 100 patients were used for validation analysis. Total RNA from those tissues was prepared with the RNeasy Mini Kit together with RNase-free DNase (Qiagen, Hiden, Germany). The integrity of the RNA obtained was assessed by an Agilent 2100 BioAnalyzer (Agilent Technologies, Palo Alto, CA, USA). All samples had a RNA integrity number (RIN) of >5.0. Using 2 μg of total RNA specimen tissues, cRNAs were prepared with a one-cycle target labeling and control reagents kit (Affymetrix, Santa Clara, CA, USA), and the microarray hybridization was carried out on Human Genome U133 2.0 chips (Affymetrix) according to the manufacturer's protocol.

Analysis of Gene Expression Data

A total of 42 training microarray data sets, including 15 HCC cases associated with HBV infection and 27 HCC cases associated with HCV infection, were normalized by the robust multiarray average (RMA) method by R statistical software, version 2.12.1, with the BioConductor package. Estimated gene expression levels were obtained in log2-transformed values, and 62 control probe sets were removed for further analysis. The fold change (FC) values were calculated by the ratio of the geometric means of the gene expression levels between the well-differentiated and poorly differentiated groups. A Wilcoxon rank sum test was performed to estimate the significance levels of the differences in gene expression between the two groups. A hierarchical clustering with the selected genes was performed with R software using the Euclidean distance and complete linkage method.

Quantitative Real-Time Polymerase Chain Reaction (RT-PCR)

A total of 2 μg of tissue RNA was reverse transcribed to cDNA with a high-capacity cDNA reverse transcription kit (Applied Biosystems) according to the manufacturer's

instructions. The TaqMan MGB probe for PTP4A3/PRL-3 (Hs02341135_m1) was used for gene expression assays, and each PCR reaction was repeated at least three times. For the quantitative analysis of specific mRNA expression, CT values were calculated by 7500 SDS software. The data were analyzed by the ΔΔCT method (Applied Biosystems User Bulletin 2, 1997), and 18S rRNA was used as an internal control.

Preparation of Cell Lines and RT-PCR of PTP4A3/PRL-3 mRNA

The human hepatoma cell lines SK-Hep1, Hep3-B, and PLC/PRF/5 were kindly provided by the American Type Culture Collection (Manassas, VA, USA). Huh1, Huh6, Huh7, HLE, HLF, HepG2, JHH1, JHH2, JHH4, and JHH5 were obtained from the Human Science Research Resources Bank (Osaka, Japan). The conditions of cell culture were reported previously.[24] Total RNA was extracted with the RNeasy Mini Kit and reverse transcribed to cDNA with a high-capacity cDNA reverse transcription kit according to the manufacturer's instructions.

Immunohistochemical Staining

To further validate the expression of the candidate gene by microarray, immunohistochemical studies were performed. The primary antibody used was a polyclonal rabbit anti-human PTP4A3 (ab50276, Abcam, Cambridge, UK), diluted 1:400 in phosphate-buffered saline containing 1 % bovine serum albumin. The tissue sections were stained with an automated immunostainer (BenchMark XT; Ventana Medical Systems, Tucson, AZ, USA) by using heat-induced epitope retrieval and a standard diaminobenzidine detection kit (Ventana). The intensity of the cytoplasmic and nuclear membrane immunostaining for PTP4A3/PRL-3 was graded as follows: 0, no immunostaining; 1, immunostaining observed in <20 % of tumor cells; 2, moderate immunostaining observed in 20–49 %; and 3, strong and diffuse immunostaining observed in >50 % of tumor cells. A score of 0 or 1 was considered negative, whereas scores of 2 or 3 were considered positive. The immunohistochemical staining was evaluated under a light microscope by two independent investigators.

Statistical Analysis

Statistical comparisons of the clinicopathological characteristics were performed by the χ^2 test or Fisher's exact test. Differences in mRNA levels between groups and the association between clinicopathological factors were analyzed by the Student t test. The data were expressed as mean ± standard deviation (SD). Fisher's exact test was performed to estimate the associated between gene expression and the clinicopathological variables in each group. Overall survival (OS) and recurrence-free survival (RFS) curves were obtained by the Kaplan–Meier method and were compared with the log-rank test. Univariate and multivariate analyses were performed by Cox proportional hazard models.

RESULTS

Strong Expression of PTP4A3/PRL-3 in of Poorly Differentiated Tumors was Detected by Gene Expression Profiling

Identification of those genes associated with the differentiation of the HCCs was performed by using the gene expression profiles obtained by the DNA microarray. First, the gene expression analysis was performed for 15 HCC cases associated with HBV (Fig. 1a) and 27 HCCs associated with HCV (Fig. 1b) according to a well or poor differentiation status of the tumor, respectively. In 54,613 probe sets, 32 probes (associated with HBV cases) (Supplementary Table S2) and 160 probes (associated with HCV cases) (Supplementary Table S3) that satisfied Wilcoxon $P < 0.005$ and FC > 3.0 were identified as differently expressed genes. As shown in Fig. 1a, b, the tumors were clearly divided by hierarchical clustering for well-differentiated (green) versus poorly differentiated (orange) cases. Next, we selected five probes (four genes) that had similar expression patterns associated with tumor differentiation, and the hepatic background was also associated HBV or HCV ($P < 0.005$, FC > 3.0) (Supplementary Table S4). Interestingly, the PTP4A3/PRL-3 gene was significantly upregulated in the poorly differentiated tumors in both HBV- and HCV-associated cases, indicating that PTP4A3/PRL-3 was the dominant molecule in the poorly differentiated HCC tumors. We then investigated the cumulative OS and tumor RFS curves of the 42 training cases for PTP4A3/PRL-3 expression after curative surgery. There were significant differences between the PTP4A3/PRL-3 high and low expression groups in terms of the OS ($P = 0.0021$) and RFS ($P = 0.0106$) rate, respectively (Fig. 1c, d).

Clinicopathological and Molecular Factors Associated with HCC Survival and Recurrence

We examined the association between the clinicopathological factors and survivals of the 42 training patients with primary HCCs. The clinicopathological features of the 42 training patients according their differentiation status were studied by statistical analyses (Supplementary Table S1). The univariate Cox regression analysis demonstrated that the prothrombin time, AFP, portal vein invasion, advanced cancer stages, poor differentiation, and higher PTP4A3/PRL-3 expression correlated with both cumulative OS and RFS. The aspartate amino transferase (AST) and hepatic vein invasion correlated only with RFS. The other clinicopathological factors were not statistically significant (Table 1).

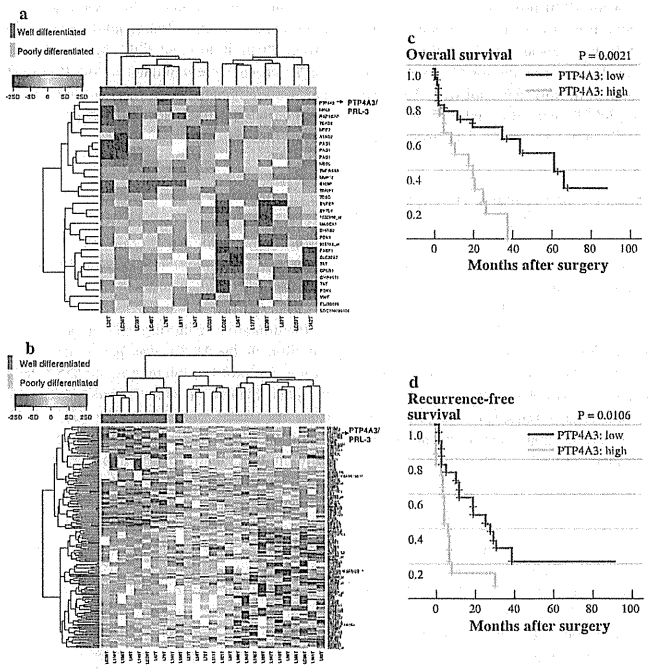

FIG. 1 Microarray analysis of human hepatocellular carcinoma. **a** Hierarchical clustering of the gene expression for well-differentiated (*green*) and poorly differentiated (*orange*) HBV-associated HCC samples. **b** Hierarchical clustering of HCV-associated HCC samples. These genes were identified by the Wilcoxon signed rank test ($P < 0.005$), and a more than three-fold change between the two groups of well versus poorly differentiated HCCs. *Red* and *blue* represent relative overexpression and underexpression, respectively. **c**, **d** OS and RFS of 42 postoperative HCC patients associated with the expression of the PTP4A3/PRL-3 gene in cancerous liver tissue. The mean expression level for each gene was used as a cutoff value. *Solid* or *dotted lines* indicate the Kaplan–Meier curves for patients with relative overexpression and underexpression, respectively. The log-rank test was used to assess the statistical difference between the two groups (OS, $P = 0.0021$; RFS, $P = 0.0106$). *HBV* hepatitis B virus, *HCC* hepatocellular carcinoma, *HCV* hepatitis C virus, *OS* overall survival, *RFS* recurrence-free survival

Validation Study by TaqMan Gene Expression Assays

According to the training microarray analysis, the PTP4A3/PRL-3 gene was closely correlated with poor differentiation, poorer OS, and recurrence of HCC. To confirm the microarray findings, the results were independently validated by TaqMan gene expression assays. We also tested the microarray results in training sets. There was a significant correlation between the cDNA microarray and TaqMan gene expression assays results in terms of PTP4A3/PRL-3 expression (Fig. 2a). The expression of PTP4A3/PRL-3 in poorly differentiated HCC tissues was significantly higher than in well-differentiated tissues of HCC patients associated with HBV ($P < 0.01$) or HCV ($P < 0.001$) (Fig. 2c). This result was validated independently in HCC tumor tissues from 83 patients and in 10 normal liver specimens. The

TABLE 1 Cox regression analysis of the overall and recurrence-free survival in the 42 training cases

	Overall survival		Recurrence-free survival	
	Univariate HR (95 % CI)	*P*	Univariate HR (95 % CI)	*P*
Clinicopathological factors				
Age (years, mean ± SD)	0.978 (0.942–1.015)	0.2392	0.990 (0.951–1.031)	0.6367
Gender (female vs. male)	0.830 (0.331–2.212)	0.7089	0.907 (0.387–2.124)	0.822
Virus infection (HBV vs. HCV)	1.331 (0.606–2.923)	0.4768	0.940 (0.438–2.016)	0.8738
AST (IU/l, mean ± SD)	1.005 (0.994–1.016)	0.3639	1.011 (1.000–1.022)	0.0423
ALT (IU/l, mean ± SD)	1.003 (0990–1.016)	0.6777	1.006 (0.993–1.019)	0.3804
Plt ($\times 10^9$/l, mean ± SD)	1.026 (0.956–1.100)	0.4811	1.025 (0.959–1.094)	0.468
ICG-R15 (%, mean ± SD)	1.006 (0.976–1.037)	0.6863	1.016 (0.986–1.046)	0.3063
PT (%, mean ± SD)	0.945 (0.913–0.978)	0.0013	0.967 (0.937–0.998)	0.0396
T. bil (mg/dl, mean ± SD)	1.942 (1.165–3.237)	0.0109	1.144 (0.649–2.018)	0.6411
Alb (g/dl, mean ± SD)	0.624 (0.289–1.348)	0.2302	0.690 (0.326–1.458)	0.3311
AFP (ng/ml, log10)	1.769 (1.312–2.385)	0.0002	1.767 (1.338–2.332)	<0.0001
PIVKA-II (mAU/ml, log10)	1.196 (0.827–1.730)	0.3411	1.282 (0.891–1.846)	0.1813
Tumor max size (cm, mean ± SD)	1.092 (0.957–1.246)	0.1900	1.105 (0.982–1.243)	0.0965
Multiple versus solitary	0.936 (0.376–2.332)	0.8870	1.305 (0.577–2.954)	0.5227
Capsular formation (−) versus (+)	1.632 (0.761–3.501)	0.2083	0.902 (0.413–1.974)	0.7968
Capsular invasion (−) versus (+)	1.752 (0.814–3.772)	0.1517	1.295 (0.615–2.726)	0.4967
Portal vein invasion (pvp)	0.307 (0.138–0.683)	0.0038	0.185 (0.084–0.405)	<0.0001
Hepatic vein invasion (pvv)	0.663 (0.244–1.806)	0.4212	0.374 (0.156–0.897)	0.0276
Vascular invasion (pvp/pvv)	0.331 (0.114–0.777)	0.0112	0.179 (0.080–0.400)	<0.0001
Stage (III + IV) versus (I + II)	0.331 (0.114–0.777)	0.0112	0.344 (0.160–0.740)	0.0063
Degree of differentiation (poor vs. well)	4.146 (1.526–11.263)	0.0053	3.678 (1.596–8.477)	0.0022
Molecule factor				
PTP4A3/PRL-3 expression (high)	3.563 (1.5.09–8.411)	0.0037	2.598 (1.217–5.545)	0.0136

HR hazard ratio, *CI* confidence interval, *HBV* hepatitis B virus, *HCV* hepatitis C virus, *AST* aspartate amino transferase, *ALT* alanine amino-transferase, *PLT* platelet, *ICG-R15* indocyanine green retention rate at 15 min, *PT* prothrombin time, *T. bil* total bilirubin, *Alb* albumin, *AFP* α-fetoprotein, *PIVKA-II* protein induced by vitamin K absence or antagonists II

mRNA expression levels of PTP4A3/PRL-3 were statistically significantly different between HCC and normal liver specimens (5.29 ± 1.43 vs. 3.86 ± 0.76, $P = 0.0035$, Fig. 3b, left), PTP4A3/PRL-3 was more highly expressed in poorly differentiated disease than in well-differentiated disease (6.21 ± 2.25 vs. 4.17 ± 1.70, $P < 0.0001$, Fig. 3b, right). The clinicopathological significance of PTP4A3/PRL-3 mRNA expression was also analyzed. Depending on the expression level (means ± SD) of PTP4A3/PRL-3 mRNA, the clinicopathological factors were divided into two groups. PTP4A3/PRL-3 mRNA was significantly correlated with virus infection ($P = 0.0422$), serum AFP ($P = 0.0047$), PIVKA-II ($P = 0.0259$), portal vein invasion ($P = 0.0156$), and vascular invasion ($P = 0.0192$) (Table 2). There were no statistically significant differences between age, gender, size of tumor, number of tumors, tumor infiltration into the capsule, and stages of the tumor.

Expression of PTP4A3/PRL-3 in HCC Cell Lines

The expression level of PTP4A3/PRL-3 mRNA was evaluated in 13 hepatoma cell lines. The PTP4A3/PRL-3 mRNA was highly expressed in HCC cell lines, and there were different expression patterns (Fig. 3c). In 2 of 13 cells, the PTP4A3/PRL-3 mRNA levels were lower than in the known cell lines such as HLE and HLF derived from epithelial and fibroblastic colonies in cultures of the same undifferentiated hepatomas and did not produce AFP and albumin. The other cells were derived from differentiated hepatomas and produced AFP.

Immunohistochemical Detection of PTP4A3/PRL-3 in HCC Tissues and Association with Clinicopathological Variables

Next, an immunohistochemical analysis was performed for the evaluation of the clinical significance of

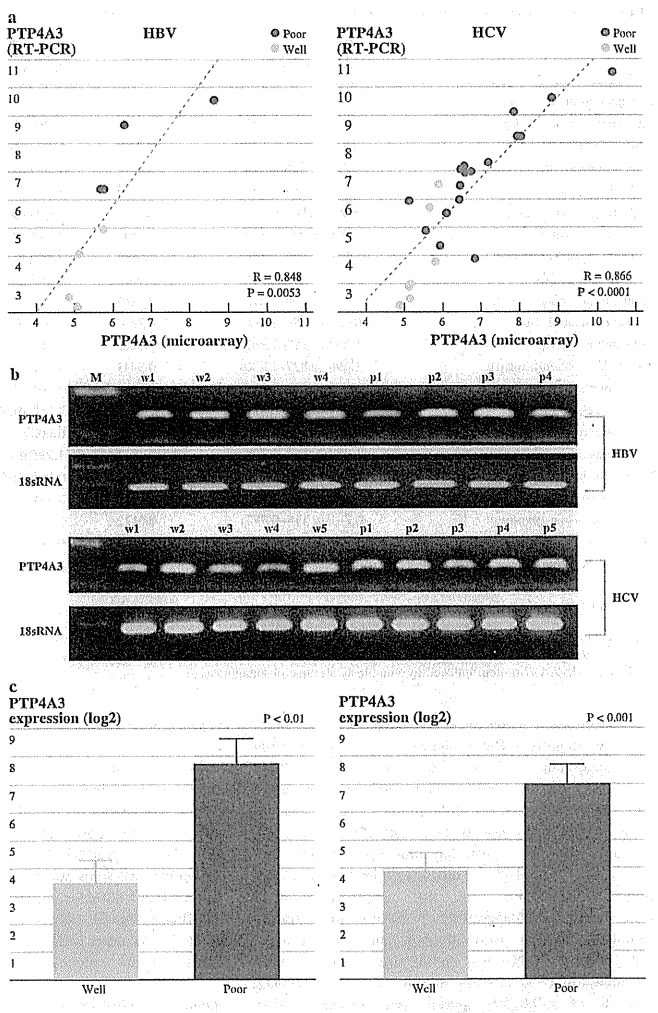

FIG. 2 Training study: expression of PTP4A3/PRL-3 in HCC. **a** Correlation of the test samples for PTP4A3/PRL-3 mRNA expression by cDNA microarray and TaqMan gene expression assays (*left* HBV-associated patients, *right* HCV-associated patients). **b** RT-PCR products were detected by agarose gel electrophoreses stratified by HBV- or HCV-associated HCC. (*w* Well-differentiated, *p* poorly differentiated). **c** The mRNA expression levels of PTP4A3/PRL-3 were compared between poorly differentiated and well-differentiated disease according to the presence of HBV (*left*) associated ($P < 0.01$) or HCV (*right*) associated ($P < 0.001$) HCC, respectively. **d** Immunohistochemical analysis of PTP4A3/PRL-3 in HCC tissues from the test samples. *Top* HE staining. *Middle*, *bottom* PTP4A3/PRL-3-high (*right*) or low (*left*) expression (original magnification, ×100, ×200)

PTP4A3/PRL-3 expression by using tissue samples from 100 patients with HCC. We also tested the immunoreactivity of PTP4A3/PRL-3 in the same microarray test samples. The results for PTP4A3/PRL-3 immunostaining are shown in Fig. 2d. PTP4A3/PRL-3 protein was mainly localized in the cytoplasm and nuclear membrane of the cancer cells, and rarely nuclear staining was also seen. Consequently, the specific overexpression of PTP4A3/PRL-3 was recognized in 57 of 100 cases (Fig. 3d).

FIG. 2 continued

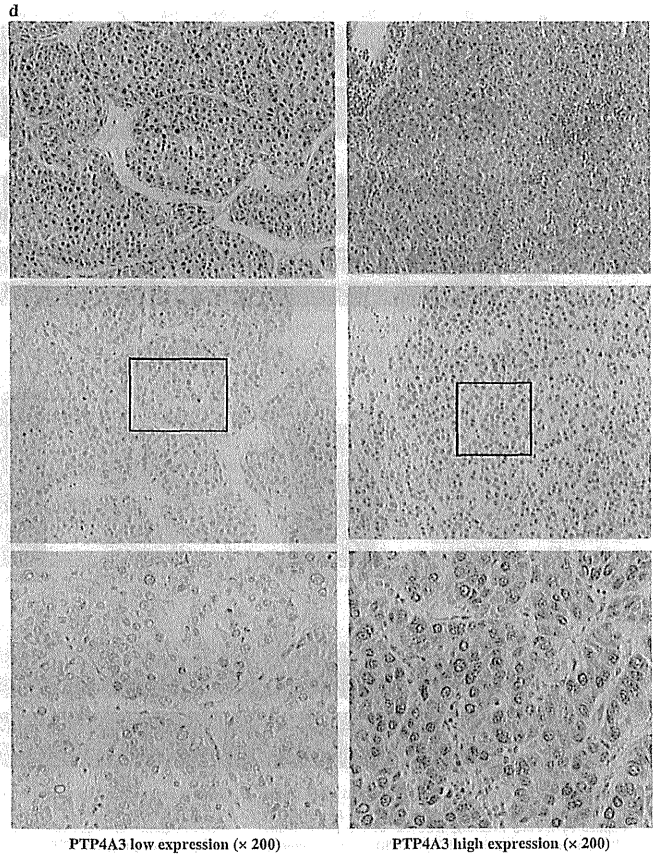

The clinicopathological significance of PTP4A3/PRL-3 expression was then evaluated in the PTP4A3/PRL-3-positive group ($n = 57$) and compared to the negative group ($n = 43$) of HCC patients (Table 2). The protein expression of PTP4A3/PRL-3 was significantly correlated with tumor differentiation ($P < 0.0001$), serum AFP ($P = 0.0118$), high serum PIVKA-II ($P = 0.0214$), hepatic vein invasion ($P = 0.0374$), tumor vascular invasion ($P = 0.0198$), and advanced cancer stages ($P = 0.0047$).

Overexpression of PTP4A3 Protein in HCC Tissues Associated with a Poor Prognosis

To examine the prognostic significance of PTP4A3/PRL-3 expression, we performed a validation study on 100 patients with HCC. According to the immunostaining analysis of HCC tissues, the OS and RFS survival were then compared between the two groups. The PTP4A3/PRL-3-positive group demonstrated a significantly poorer survival than the PTP4A3/PRL-3-negative group for both OS

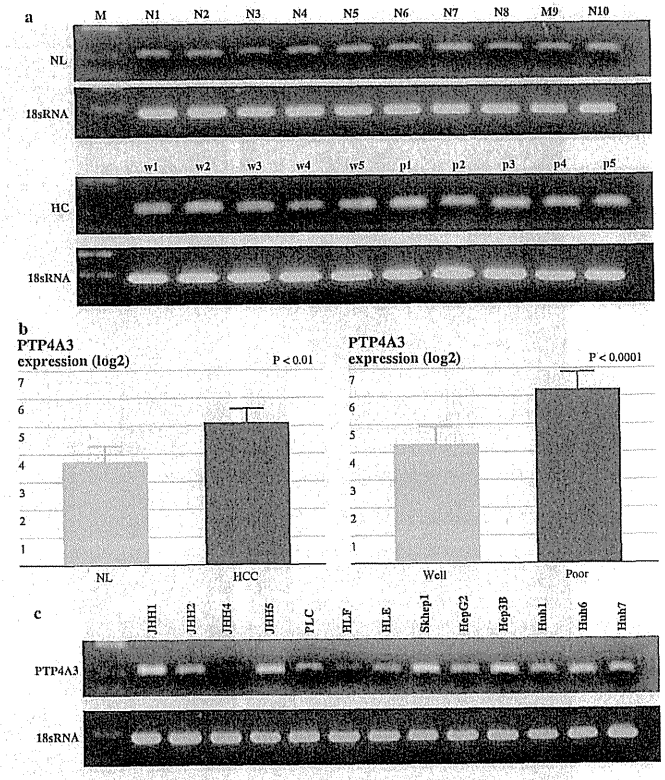

FIG. 3 Validation study: expression of PTP4A3/PRL-3 in human HCC. **a** RT-PCR products were detected by agarose gel electrophoreses stratified by normal liver and HCC (*w* well, *p* poor) tissues. **b** The mRNA expression levels of PTP4A3/PRL-3 were compared between the HCC and normal liver tissues (NL) ($P < 0.01$), and between well-differentiated and poorly differentiated HCC tissues ($P < 0.0001$) by TaqMan gene expression assay. **c** The expression of PTP4A3/PRL-3 in hepatoma cell lines. **d** Immunohistochemical analysis of PTP4A3/PRL-3 in HCC tissues from the validation samples. A representative positive immunostaining case (*top*) and a negative immunostaining case (*bottom*) are shown. **e** Kaplan–Meier estimates for the OS and RFS times with respect to PTP4A3/PRL-3 protein expression in primary HCCs. The survival rate of patients with positive or negative PTP4A3/PRL-3 expression are indicated by *solid* or *dotted lines*, respectively. The log-rank test results revealed a significant difference in OS rates between the two groups ($P = 0.0024$), and also a significant difference was observed for the RFS rates between the two groups ($P = 0.0227$). *HCC* hepatocellular carcinoma, *OS* overall survival, *RFS* recurrence-free survival

($P = 0.0024$) and RFS ($P = 0.0227$). We also investigated the association between the OS and RFS rates and clinicopathological factors, and we performed univariate and multivariate Cox regression analyses (Table 3). The OS was statistically significantly correlated with seven factors such as AST, serum AFP, tumor size, tumor differentiation, portal vein invasion, stage of tumor, and PTP4A3/PRL-3 expression. On the multivariate analysis, PTP4A3/PRL-3 expression (hazard ratio [HR] 0.542; $P = 0.048$), portal vein invasion (HR 0.470; $P = 0.023$), and AST (HR 1.006; $P = 0.048$) were statistically significant prognostic factors for OS, but not for the RFS rate (Table 3).

FIG. 3 continued

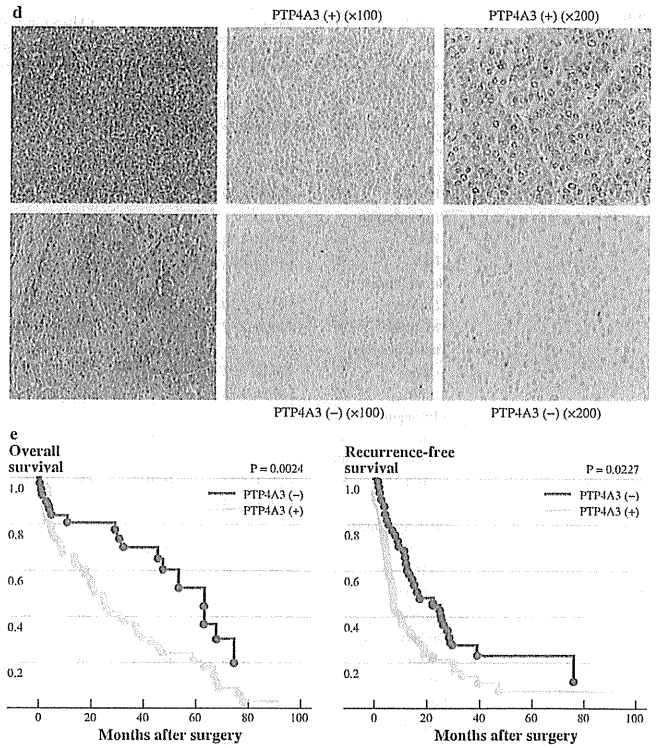

DISCUSSION

In the present study, the gene expression profiles of PTP4A3/PRL-3 were obtained in poorly differentiated and well-differentiated HCC, regardless of the background of the virus. On the basis of the training analysis, strong PTP4A3/PRL-3 expression was significantly correlated with the cumulative survival and recurrence-free rates of the patients (Fig. 1c, d; Table 1). This result was validated independently by TaqMan gene expression assays and immunostaining. We also studied the significance of PTP4A3/PRL-3 mRNA and protein expression, from a clinical viewpoint, for the progression of HCC. The overexpression of PTP4A3/PRL-3 was significantly correlated with the serum levels of AFP and PIVKA-II, tumor vascular invasion, and advanced cancer stages in HCC patients. Similar results have been reported by Zhao et al.,[22] suggesting that PRL-3 expression was correlated with angiogenesis and invasion through an upregulation of matrix metalloproteinases (MMPs) or a downregulation of E-cadherin by using limited HCC cases. PRL-3 expression has also been reported in colon, breast, ovarian, and gastric cancers, where its presence seems to have an important role in the acquisition of metastatic potential.[11,15–21] In our studies, the clinical significance of PTP4A3/PRL-3 expression was noted and correlated significantly with poor tumor differentiation ($P < 0.0001$) and the OS and RFS of HCC patients (Fig. 3e). PTP4A3/PRL-3 expression also showed a significant correlation with a poor clinical outcome (Table 3).

PTP4A3/PRL-3 plays multiple roles in cancer metastasis. By activating a series of intracellular signaling pathways, PRL-3 induces cell differentiation, proliferation, invasion, and metastasis.[7–9] Invasion through the basement membrane and interstitial extracellular matrix is another key event for metastatic progression, which requires the action of a series of proteolytic enzymes, the MMPs. The MMP family is closely correlated with metastatic potential;

TABLE 2 Association between PTP4A3/PRL-3 expression and clinicopathological factors in HCC patients

Variable	PTP4A3 mRNA			PTP4A3 protein			
	n	Mean ± SD	*P*	*n*	Negative	Positive	*P*
Age (years)							
<60	20	5.10 ± 2.23	0.9009	28	11	17	0.6609
≥60	63	5.17 ± 2.23		72	32	40	
Gender							
Male	60	5.32 ± 2.38	0.2895	72	25	47	0.0126
Female	23	4.74 ± 1.70		28	18	10	
Virus infection							
HBV	25	4.40 ± 2.46	0.0422	33	18	15	0.1333
HCV	58	5.48 ± 2.05		67	25	42	
No. of tumors							
Solitary	53	5.13 ± 2.10	0.8942	71	33	38	0.3736
Multiple	30	5.20 ± 2.47		29	10	19	
Tumor size (cm)							
<5.0	58	4.86 ± 1.92	0.0706	70	33	37	0.2710
≥5.0	25	5.83 ± 2.73		30	10	20	
AFP (ng/ml)							
<20	34	4.22 ± 1.85	0.0011	40	26	14	0.0004
≥20	49	5.80 ± 2.24		60	17	43	
<100	55	4.67 ± 2.07	0.0047	65	34	31	0.0118
≥100	28	6.11 ± 2.23		35	9	26	
PIVKA-II (mAU/ml)							
<100	39	4.58 ± 2.38	0.0259	46	23	23	0.2268
≥100	44	5.66 ± 1.96		54	20	34	
<1000	59	4.82 ± 2.16	0.0313	74	37	37	0.0214
≥1000	24	5.97 ± 2.20		26	6	20	
Differentiation							
Well	43	4.17 ± 1.70	<0.0001	46	30	16	<0.0001
Poor	40	6.21 ± 2.25		54	13	41	
Infiltration to capsule (fc-inf)							
Absent	35	5.30 ± 2.49	0.6177	48	20	28	0.8416
Present	48	5.05 ± 2.02		52	23	29	
Portal vein invasion (pvp)							
Absent	60	4.79 ± 2.21	0.0156	72	35	37	0.0770
Present	23	6.10 ± 2.00		28	8	20	
Hepatic vein invasion (pvv)							
Absent	71	5.00 ± 2.28	0.1310	87	41	46	0.0374
Present	12	6.05 ± 1.65		13	2	11	
Vascular invasion (pvp/pvv)							
Absent	53	4.73 ± 2.28	0.0192	66	34	32	0.0198
Present	30	5.91 ± 1.93		34	9	25	
Tumor stages							
I + II	33	4.75 ± 1.83	0.1795	44	26	18	0.0047
III + IV	50	5.42 ± 2.43		56	17	39	

HBV hepatitis B virus, *HCV* hepatitis C virus, *AFP* α-fetoprotein, *PIVKA-II* protein induced by vitamin K absence or antagonists II

TABLE 3 Cox regression analysis of overall and recurrence-free survival in 100 validation cases

	Overall survival				Recurrence-free survival			
	Univariate analysis		Variable selection		Univariate analysis		Variable selection	
	HR (95 % CI)	*P*	HR (95 % CI)	*P*	HR (95 % CI)	*P*	HR (95 % CI)	*P*
Clinicopathological factors								
Age (years, mean ± SD)	0.996 (0.968–1.025)	0.7901			0.993 (0.966–1.021)	0.6375		
Gender (female/male)	0.712 (0.412–1.229)	0.2226			0.755 (0.456–1.250)	0.2752		
Virus infection (HBV vs. HCV)	1.142 (0.673–1.938)	0.6231			1.187 (0.730–1.931)	0.4892		
AST (IU/l, mean ± SD)	1.007 (1.001–1.014)	0.0192	1.006 (1.000–1.013)	0.048	1.005 (0.998–1.012)	0.1327		
ALT (IU/l, mean ± SD)	1.005 (0.999–1.011)	0.1096			1.004 (0.997–1.010)	0.2977		
Plt ($\times 10^9$/l, mean ± SD)	1.017 (0.987–1.047)	0.2822			0.999 (0.970–1.030)	0.9601		
ICG-R15 (%, mean ± SD)	0.997 (0.979–1.015)	0.7119			0.998 (0.982–1.015)	0.8202		
PT (%, mean ± SD)	0.991 (0.978–1.005)	0.2113			0.996 (0.984–1.008)	0.4896		
T. bil (mg/dl, mean ± SD)	1.212 (0.859–1.709)	0.2741			0.964 (0.676–1.369)	0.838		
Alb (g/dl, mean ± SD)	1.062 (0.756–1.491)	0.7287			0.973 (0.732–1.293)	0.8495		
AFP, ng/ml (≥20 vs. <20)	0.523 (0.309–0.885)	0.0157	0.939 (0.526–1.676)	0.832	0.505 (0.308–0.827)	0.0067	0.815 (0.453–1.466)	0.4946
PIVKA-II, mAU/ml (≥40 vs.<40)	0.842 (0.509–1.391)	0.5009			1.091 (0.681–1.749)	0.7161		
Maximum tumor size (cm, mean ± SD)	1.149 (1.055–1.252)	0.0014	1.064 (0.956–1.185)	0.2544	1.111 (1.023–1.207)	0.0127	0.952 (0.847–1.071)	0.4127
No. of tumors (multiple vs. solitary)	0.836 (0.483–1.515)	0.5930			1.312 (0.796–2.165)	0.2869		
Differentiation (poor vs. well)	2.364 (1.412–3.968)	0.0011	1.266 (0.661–2.424)	0.477	1.931 (1.206–3.094)	0.0066	1.026 (0.562–1.872)	0.9345
Capsular invasion (pfc-inf) (∓)	1.344 (0.822–2.197)	0.2388			1.192 (0.750–1.893)	0.4583		
Portal vein invasion	0.304 (0.177–0.523)	<0.0001	0.470 (0.245–0.901)	0.023	0.251 (0.150–0.420)	<0.0001	0.316 (0.165–0.603)	0.0005
Hepatic vein invasion	0.823 (0.403–1.682)	0.5933			0.472 (0.253–0.879)	0.0181	0.654 (0.326–1.312)	0.2321
Stage (III + IV) versus (I + II)	0.400 (0.239–0.658)	0.0005	0.661 (0.352–1.239)	0.196	0.410 (0.253–0.664)	0.0003	0.489 (0.269–0.890)	0.0191
Molecular factor								
PTP4A3/PRL-3 protein expression	0.440 (0.255–0.759)	0.0031	0.542 (0.294–0.997)	0.048	0.578 (0.359–0.932)	0.0245	1.000 (0.556–1.798)	0.9994

HR hazard ratio, *CI* confidence interval, *HBV* hepatitis B virus, *HCV* hepatitis C virus, *AST* aspartate amino transferase, *ALT* alanine amino-transferase, *PLT* platelet, *PT* prothrombin time, *ICG-R15* indocyanine green retention rate at 15 min, *T. bil* total bilirubin, *Alb* albumin, *AFP* α-fetoprotein, *PIVKA-II* protein induced by vitamin K absence or antagonists II

they can degrade denatured collagens and type IV collagen present in the basement membrane.[25] In our training microarray studies (Supplementary Table S2), MMP12 was also highly expressed in poorly differentiated patients with HCC. In addition, other members of the metalloproteinase family such as MMP1, MMP9, and MMP10 (Wilcoxon $P < 0.05$; FC > 1.5) were also upregulated in poorly differentiated patients (data not shown in Supplementary Table S2). We found significantly positive correlations between PTP4A3/PRL-3 and MMP12 ($r = 0.721, P < 0.0001$), MMP1 ($r = 0.514$, $P = 0.0004$), MMP9 ($r = 0.501$, $P = 0.0006$), and MMP10 ($r = 0.347, P = 0.0236$) (Supplementary Fig. S1). Several studies have suggested that a downregulation of E-cadherin-mediated intercellular adhesion increased tumor differentiation, invasion, and metastasis and led to a poor prognosis in human cancers, including HCC.[26,27] At present, our microarray studies also showed that the downregulation of E-cadherin in tumor tissues was associated with hepatic vascular invasion, moderate to poor differentiation, and the recurrence of patients with HCC (data not shown). However, there was no statistical correlation between PTP4A3/PRL-3 expression and E-cadherin expression on the basis of the training sets analysis (Supplementary Fig. S1). This result suggested a role for PTP4A3/PRL-3 overexpression in HCC, and its ectopic expression in different cell types is correlated with the induction of metastatic phenotypes, such as invasion and motility capabilities. PTP4A3/PRL-3 expression was predominantly correlated with poorly differentiated tumor cells and increased invasion potential through an upregulation of MMPs.

In the present study, we showed that PTP4A3/PRL-3 was predominantly localized in the cytoplasm and nuclear membrane by immunostaining. The expression of membrane-associated PRL-3 may induce a dephosphorylation of target substrates at the cell membrane, thus modulating the organization of the plasma membrane in such a way to promote cell motility and invasion.[8] The membrane structures associated with PRL-3 including ruffles, protrusions, and some vacuolar-like membrane extensions could represent another opportunity for intervention. These membrane structures have been demonstrated to play a role in cell movement and invasion.[28]

Several recent studies have demonstrated the capability of PRL-3 to regulate multiple signaling cascades, including the PI3K-Akt, Rho, and Csk/Src pathways, which are crucial for both cell cycle progression and cell migration.[29,30] PRL-3-enhanced cell migration is dependent on the preservation of its catalytic function, and the consensus phosphatase motif will potentially be a therapeutic target. Prenylation-dependent association could effectively block the function of PRL-3 in cell migration and invasion.[8] Aberrant PTP4A3/PRL-3 expression may be closely related to poor tumor differentiation, tumor invasion, and poorer survival in HCC patients, and this accelerated hepatocarcinogenesis may be positively regulated by hepatoepithelial cell migration, thus promoting tumor progression and the establishment of the new vasculature needed for tumor survival and expansion. However, at this time, we are not able to analyze any data to support this hypothesis. Further study is required to verify these possibilities.

In conclusion, PTP4A3/PRL-3 was identified as one of the overexpressed molecules in HCC tissues. PTP4A3/PRL-3 might be closely associated with HCC progression, invasion, and metastasis, and its strong expression had a negative impact on the prognosis of HCC patients. This suggests that PRL-3 should be considered as a prognostic factor. Further attention should be paid to abnormalities in phosphatase of PRL-3 in HCC progression as a potential target for therapy.

ACKNOWLEDGMENT The authors thank Hiromi Onari and Ayumi Shioya for clerical and technical assistance. This work was supported by Special Coordination Funds for Promoting Science and Technology (Japan Science and Technology Agency), and a grant-in-aid from the Ministry of Education, Culture, Sports, Science and Technology of Japan.

REFERENCES

1. Parkin DM, Bray F, Ferlay J, Pisani P. Global cancer statistics, 2002. *CA Cancer J Clin.* 2005;55:74–108.
2. Shimada K, Sano T, Sakamoto Y, et al. A long-term follow-up and management study of hepatocellular carcinoma patients surviving for 10 years or longer after curative hepatectomy. *Cancer.* 2005;104:1939–47.
3. Song TJ, Ip EW, Fong Y. Hepatocellular carcinoma. Current surgical management. *Gastroenterology.* 2004;127:248–60.
4. Cates CA, Michael RL, Stayrook KR. Prenylation of oncogenic human PTP (CAAX) protein tyrosine phosphatases. *Cancer Lett.* 1996;110:49–55.
5. Burridge K, Sastry SK, Sallee JL. Regulation of cell adhesion by protein-tyrosine phosphatases in cell–matrix adhesion. *J Biol Chem.* 2006;281:15593–6.
6. Werner SR, Lee PA, DeCamp MW, Crowell DN, Randall SK, Crowell PL. Enhanced cell cycle progression and down regulation of p21Cip1/Waf1 by PRL tyrosine phosphatases. *Cancer Lett.* 2003;202:201–11.
7. Guo K, Li J, Tang JP, Koh V, Gan BQ, Zeng Q. Catalytic domain of PRL-3 plays an essential role in tumor metastasis, formation of PRL-3 tumors inside the blood vessel. *Cancer Biol Ther.* 2004;3:945–51.
8. Zeng Q, Dong JM, Guo K, et al. PRL-3 and PRL-1 promote cell migration, invasion, and metastasis. *Cancer Res.* 2003;63:2716–22.
9. Matter WF, Estridge T, Zhang C, et al. Role of PRL-3, a human muscle-specific tyrosine phosphatase, in angiotensin-II signaling. *Biochem Biophys Res Commun.* 2001;283:1061–8.
10. Bardelli A, Saha S, Sager JA, et al. PRL-3 expression in metastatic cancers. *Clin Cancer Res.* 2003;9:5607–15.

11. Saha S, Bardelli A, Buckhaults P, et al. A phosphatase associated with metastasis of colorectal cancer. *Science.* 2001;294:1343–6.
12. Zeng Q, Hong W, Tan YH. Mouse PRL-2 and PRL-3, two potentially prenylated protein tyrosine phosphatases homologous to PRL-1. *Biochem Biophys Res Commun.* 1998;244:421–7.
13. Zeng Q, Si X, Horstmann H, Xu Y, Hong W, Pallen CJ. Prenylation-dependent association of protein-tyrosine phosphatases PRL-1, -2, and -3 with the plasma membrane and the early endosome. *J Biol Chem.* 2000;275:21444–52.
14. Wang L, Peng L, Dong B, et al. Overexpression of phosphatase of regenerating liver-3 in breast cancer: association with a poor clinical outcome. *Ann Oncol.* 2006;17:1517–22.
15. Polato F, Codegoni A, Fruscio R, et al. PRL-3 phosphatase is implicated in ovarian cancer growth. *Clin Cancer Res.* 2005; 11:6835–9.
16. Ren T, Jiang B, Xing X, et al. Prognostic significance of phosphatase of regenerating liver-3 expression in ovarian cancer. *Pathol Oncol Res.* 2009;15:555–60.
17. Miskad UA, Semba S, Kato H, et al. High PRL-3 expression in human gastric cancer is a marker of metastasis and grades of malignancies: an in situ hybridization study. *Virchows Arch.* 2007;450:303–10.
18. Dai N, Lu AP, Shou CC, Li JY. Expression of phosphatase regenerating liver 3 is an independent prognostic indicator for gastric cancer. *World J Gastroenterol.* 2009;28:1499–505.
19. Xu Y, Zhu M, Zhang S, Liu H, Li T, Qin C. Expression and prognostic value of PRL-3 in human intrahepatic cholangiocarcinoma. *Pathol Oncol Res.* 2010;16:169–75.
20. Ooki A, Yamashita K, Kikuchi S, Sakuramoto S, Katada N, Watanabe M. Phosphatase of regenerating liver-3 as a convergent therapeutic target for lymph node metastasis in esophageal squamous cell carcinoma. *Int J Cancer.* 2010;127:543–54.
21. Ma Y, Li B. Expression of phosphatase of regenerating liver-3 in squamous cell carcinoma of the cervix. *Med Oncol.* 2011;28: 775–80.
22. Zhao WB, Li Y, Liu X, Zhang LY, Wang X. Evaluation of PRL-3 expression, and its correlation with angiogenesis and invasion in hepatocellular carcinoma. *Int J Mol Med.* 2008;22:187–92.
23. Thomas MB, Abbruzzese JL. Opportunities for targeted therapies in hepatocellular carcinoma. *J Clin Oncol.* 2005;23:8093–108.
24. Yasen M, Mizushima H, Mogushi K, et al. Expression of Aurora B and alternative forms in hepatocellular carcinoma and adjacent tissue. *Cancer Sci.* 2009;100:472–80.
25. Egeblad M, Werb Z. New functions for the matrix metalloproteinases in cancer progression. *Nat Rev Cancer.* 2002;2:161–74.
26. Endo K, Ueda T, Ueyama J, Ohta T, Terada T. Immunoreactive E-cadherin, alpha-catenin, beta-catenin, and gammacatenin proteins in hepatocellular carcinoma: relationships with tumor grade, clinicopathologic parameters, and patients' survival. *Hum Pathol.* 2000;31:558–65.
27. Matsumura T, Makino R, Mitamura K. Frequent downregulation of E-cadherin by genetic and epigenetic changes in the malignant progression of hepatocellular carcinomas. *Clin Cancer Res.* 2001;7:594–9.
28. Nobes CD, Hall A. Rho GTPases control polarity, protrusion, and adhesion during cell movement. *J Cell Biol.* 1999;144:1235–44.
29. Wang H, Quah SY, Dong JM, Manser E, Tang JP, Zeng Q. PRL-3 down-regulates PTEN expression and signals through PI3K to promote epithelial-mesenchymal transition. *Cancer Res.* 2007;67:2922–6.
30. Liang F, Liang J, Wang WQ, Sun JP, Udho E, Zhang ZY. PRL3 promotes cell invasion and proliferation by down-regulation of Csk leading to Src activation. *J Biol Chem.* 2007;282:5413–9.

IJC
International Journal of Cancer

Gene expression changes in initiation and progression of oral squamous cell carcinomas revealed by laser microdissection and oligonucleotide microarray analysis

Jun Sumino[1], Narikazu Uzawa[1], Norihiko Okada[2], Ken Miyaguchi[3], Kaoru Mogushi[3], Ken-Ichiro Takahashi[1], Hiroaki Sato[1], Chieko Michikawa[1], Yoshimi Nakata[1], Hiroshi Tanaka[3] and Teruo Amagasa[1]

[1] Maxillofacial Surgery, Maxillofacial Reconstruction and Function, Division of Maxillofacial and Neck Reconstruction, Graduate School of Medicine and Dentistry, Tokyo Medical and Dental University, Tokyo, Japan
[2] Diagnostic Oral Pathology, Oral Restitution, Division of Oral Health Science, Graduate School of Medicine and Dentistry, Tokyo Medical and Dental University, Tokyo, Japan
[3] Department of Computational Biology, Graduate School of Biomedical Science, Tokyo Medical and Dental University, Tokyo, Japan

Oral carcinogenesis is a complex process involving multiple genes. However, the genetic changes involved in this process are not apparent in identical oral squamous cell carcinomas (OSCCs). According to pathological characteristics, samples of normal tissue, oral dysplastic lesions (ODLs), and invasive cancers were obtained from identical OSCCs using laser microdissection (LMD). Large-scale gene expression profiling was carried out on 33 samples derived from 11 OSCCs. We analyzed genes differentially expressed in normal tissues *vs.* ODLs and in ODLs *vs.* invasive tumors and identified 15 candidate genes with continuously increasing or decreasing expression during oral carcinogenesis. One of these genes, *ISG15*, was chosen for further characterization. Real-time quantitative reverse transcription-polymerase chain reaction and immunohistochemical analysis confirmed that *ISG15* expression consistently increased during oral tumorigenesis. An ISG15 high-expression level was significantly associated with poor prognosis ($p = 0.027$). In addition, patients with high-expression tumors had a poorer 5-year survival rate than patients with low expression levels ($p = 0.019$). In conclusion, we identified 15 genes with continuously increasing or decreasing expression during oral carcinogenesis. One of these, *ISG15*, is likely to be associated with both dysgenesis and tumorigenesis and may be a potential prognostic marker for oral cancer.

Oral squamous cell carcinoma (OSCC) is the sixth most common malignant tumor worldwide, with an estimated incidence of 211,000–405,000 deaths annually.[1] Considerable advances in surgical and medical treatments for OSCC over the past two decades have unfortunately not improved overall disease outcome. Moreover, OSCC is often associated with significant morbidity such as eating, swallowing and speech dysfunction, disfigurement and psychological distress.[2]

The majority of OSCCs are preceded by visible changes of the oral mucosa. Oral dysplastic lesions (ODLs) affecting the oral mucosa have malignant potential. Clinically, ODLs most commonly present as a white patch (leukoplakia) but may also present as a red (erythroplakia) or a nonhomogenous lesion (erythroleukoplakia).[3] Oral leukoplakia (OLP), the best-known premalignant oral lesion, is defined by the World Health Organization (WHO) as "a white patch or plaque that cannot be characterized clinically or pathologically as any other disease."[4] The prevalence of malignant transformation of OLP varies from 0.13 to 17.5%, with observation periods ranging from 1 to 30 years.[5] Many aspects of ODLs continue to pose a challenge to clinicians. The treatment options for ODLs are limited. Broadly, there are three strategies available for treating patients with ODLs: surgical excision, conservative or active surveillance and chemoprevention. However, many patients have been overtreated, with potentially unnecessary morbidity, because it is difficult to predict accurately which ODLs will progress to cancer. Thus, the most appropriate treatment can be difficult to determine.[6] To overcome this problem, novel genetic and proteomic biomarkers are required to help improve prediction of which cases are likely to transform and to assist in decision-making with regard to treatment strategies. Understanding the molecular mechanisms of transition from normal epithelium to premalignancy and to oral invasive carcinoma is indispensable for the development of such molecular markers and of better treatment modalities and better diagnostic and preventive approaches.

Key words: oral, squamous cell carcinoma, microarray, laser microdissection, carcinogenesis, ISG15
Grant sponsor: Scientific Research from the Ministry of Education, Science, Sport and Culture, Japan; **Grant number:** 21592551
DOI: 10.1002/ijc.27702
History: Received 25 Jan 2012; Accepted 11 Jun 2012; Online 28 Jun 2012
Correspondence to: Narikazu Uzawa, Maxillofacial Surgery, Maxillofacial Reconstruction and Function, Division of Maxillofacial and Neck Reconstruction, Graduate School, Tokyo Medical and Dental University, 1-5-45 Yushima, Bunkyo-ku, Tokyo 113-8549, Japan, Tel.: +81-3-5803-5499, Fax: +81-3-5803-5500, E-mail: n-uzawa.mfs@tmd.ac.jp

What's new?
Oral epithelial dysplasia is a potentially precancerous lesion diagnosed histopathologically. More accurate markers predicting progression to invasive cancer are needed to enable better diagnosis of such lesions and more appropriate selection of aggressive treatment and closer follow-up. This is the first study to demonstrate gene expression changes during oral carcinogenesis using normal epithelial, premalignant, and carcinoma cells from the same oral cancer. The study also examined ISG15 expression at both mRNA and protein level in oral pre-malignant lesions and invasive cancers, demonstrating the association between ISG15 expression status and clinicopathological factors and patients survival.

Several studies have addressed the genetic progression of oral carcinogenesis using microarray analysis.[2,7] These studies have demonstrated the presence of transcriptional dysregulation because of accumulation of genetic alterations.[2,7] The data also suggest that premalignant lesions possess many of the alterations found in cancer before the development of a malignant phenotype and that most genetic alteration occurs before the phenotypic expression of malignancy.[7,8] However, there are some problems with the use of such microarray analyses, the most serious of which is the use of bulk tissue derived from different patients.[9] When using bulk tissue in microarray analysis, various amounts of stromal tissue are included. Thus, the gene expression profile of the premalignant and cancer cells is influenced by the difference in the number of stromal cells in the bulk tissue.[9] It has also been suggested that the contribution of stromal cell "contamination" to the genetic expression profiles of cancer cells is an important consideration for designing DNA microarray studies.[10] Therefore, obtaining normal epithelial, premalignant and carcinoma cells from the same sample seems to be required to reveal the transcription profile of the progression of oral carcinogenesis.

Laser microdissection (LMD) is a technique by which specific regions (*e.g.* tumor cells) within a tissue section are microscopically isolated from other tissue components (*e.g.* stromal cells).[11] This technique enables DNA, mRNA and protein to be analyzed from cell samples. Although the application of LMD to oral cancer has been reported recently, few studies have performed mRNA analysis using expression microarray and LMD in this malignancy.[10] Moreover, to our knowledge, the transcriptional progression in oral carcinogenesis has not been investigated using these methodologies.

Thus, the aim of the present study was to determine the transcriptional progression profile in oral carcinogenesis in the identical oral cancer samples using both LMD and expression microarray analysis.

Material and Methods

Patients and tissue samples

All clinical samples were obtained from the patients with OSCC who had undergone surgical excision at the Department of Maxillofacial Surgery, Graduate School, Tokyo Medical and Dental University (Tokyo, Japan) between 1999 and 2010. All study protocols were reviewed and approved by the Research Ethics Committee of Tokyo Medical and Dental University. Informed consent was obtained from all patients in accordance with our Institutional guidelines. Clinical staging was defined according to the International Union against Cancer TNM classification system. Tumors were classified histopathologically as poorly, moderately or well differentiated according to their cellular differentiation as defined by WHO criteria. The mode of tumor invasion at the tumor–host border was classified according to modified Jacobson criteria.[12,13] Disease-free survival (DFS) was calculated from the time of initial examination to the time of local, regional or distant recurrence of the disease or the time of last follow-up. Overall survival (OS) was calculated from the time of initial examination to the time of death or last follow-up.

Collection of target cells by LMD from frozen sections

Microarray samples of invasive tumor, adjacent dysplastic lesions and noncancerous normal tissue were collected from 11 patients with primary OSCCs. None of these patients received preoperative treatment. Before LMD, an oral pathologist (N.O.) determined the area of invasive tumor, adjacent dysplastic lesion and noncancerous normal tissue on all samples. Cancer tissue for LMD was immediately cut to 3-mm thick sections, while excluding the center of the tumor for pathological diagnosis, and embedded in Tissue-Tek OCT compound medium (Sakura, Tokyo, Japan) after resection. The sections were then fixed in liquid nitrogen and stored at −80°C. Frozen sections, 9 μm thick, were cut from the frozen samples and mounted onto a foil-coated glass slide, membrane slide (Leica Microsystems, Wezlar, Germany). Frozen sections were fixed in 70% ethanol for 30 sec and stained with hematoxylin and eosin before dehydration (5 sec each in 70, 95 and 100% ethanol). After air-drying, the sections were laser microdissected using AS LMD (Leica) (Figs. 1*a-1–a-3*).

RNA extraction and gene expression analysis using oligonucleotide microarray

Total RNA was extracted from each tissue using RNeasy Micro kit (Qiagen, Venlo, The Netherlands) according to the manufacturer's instructions. The quality of the obtained RNA was examined by Agilent 2100 Bioanalyzer (Agilent Technologies, Palo Alto, CA). Amplification and labeling of RNA

Cancer Genetics

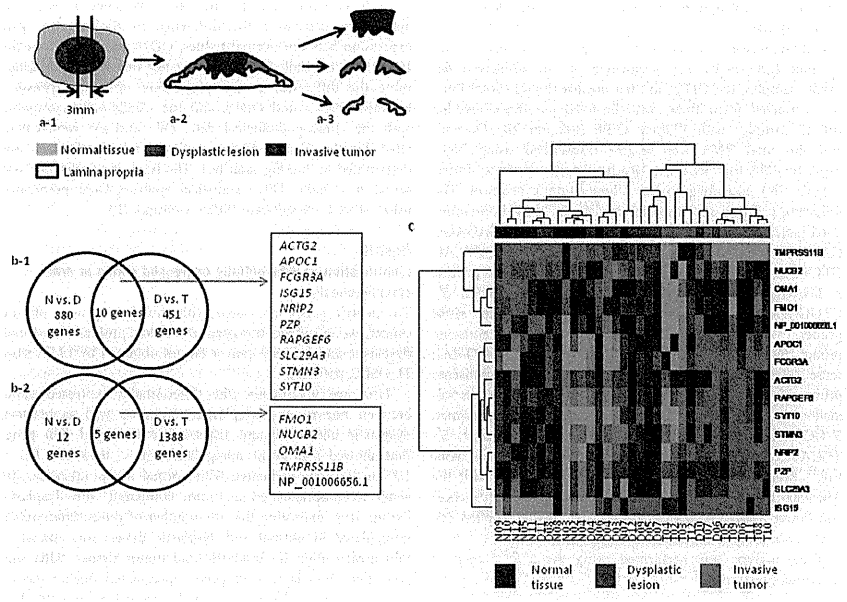

Figure 1. (*a-1*) Cancer tissue for LMD was immediately cut to 3-mm-thick section while excluding the center of cancer. (*a-2*) An oral pathologist (N.O.) determined the area of invasive tumor, dysplastic lesion and noncancerous normal tissue on all samples. (*a-3*) The sections were cut in invasive tumor, dysplastic lesion and normal tissue using a LMD system. (*b-1*) Ten genes that overlapped the 890 genes were upregulated ($p < 0.05$ and FC > 1.2) by dysplastic tissues (D) compared with normal tissues (N), and 461 genes were upregulated ($p < 0.05$ and FC > 1.2) by tumor tissues (T) compared with dysplastic tissues (D). (*b-2*) Five genes that overlapped the 17 genes were downregulated ($p < 0.05$ and FC < 0.833) by dysplastic tissues (D) compared with normal tissues (N), and 1,393 genes were downregulated ($p < 0.05$ and FC < 0.833) by tumor tissues (T) compared with dysplastic tissues (D). (*c*) Hierarchical clustering analysis using overlapping upregulated ten genes and overlapping downregulated five genes. (N) is normal tissue, (D) is dysplastic lesion and (T) is invasive tumor. Number is case number (*i.e.* N08 is normal tissue of case 8).

were performed using TargetAmp 2-Round Aminoallyl-aRNA Amplification Kit 1.0 (Epicentre, Madison, WI). Hybridization and signal detection of Human V4.0 OpArray (Operon Biotechnologies, Cologne, Germany) were then performed according to the manufacturer's instruction. The net intensity level of each spot was calculated by subtracting the background intensity from the raw intensity. Before statistical analysis, the net intensity values <1 were set to 1 and were log-2 transformed. The microarray data have been deposited at Gene Expression Omnibus (http:// www.ncbi.nlm.nih.gov/geo) under accession number GSE35261.

Profiling analyses using microarray data

For each of the 35,035 probes on the Human V4.0 OpArray, we analyzed genes differentially expressed in (*i*) normal *vs.* dysplastic tissues and (*ii*) dysplastic *vs.* tumor tissues. We used the Wilcoxon signed-rank test with a significance level of 0.05. Fold-change (FC) values were calculated using ratios of geometric means of gene expression levels in each tissue, and genes showing at least 1.2-fold difference were selected. We further selected genes that showed consistent upregulation or downregulation during tumorigenesis by examination of overlapping genes in normal *vs.* dysplastic tissues and dysplastic *vs.* tumor tissues.

To investigate the molecular characteristics of dysplastic and tumor tissues during disease progression in OSCC, we next compared the gene expression profiles of normal, dysplastic and cancerous tissues using the selected genes. Hierarchical clustering was performed using the Pearson's correlation coefficient as a similarity index and a complete linkage method for agglomeration. For visualization, gene expression levels were normalized by subtracting the mean expression level for each probe.

Quantitative real-time reverse transcription-polymerase chain reaction

Quantitative real-time reverse transcription-polymerase chain reaction (qRT-PCR) was performed on an additional ten OSCC samples, ten ODLs and ten normal tissues. Total RNA was extracted from these formalin-fixed paraffin-embedded (FFPE) samples with RNeasy FFPE isolation kit (Qiagen), and the total RNA was reverse transcribed using high-capacity RNA-to-cDNA Kit (Roche Applied Science, Indianapolis, IN) according to the manufacturer's protocol. The following primers were used to amplify the interferon-stimulated gene 15 kDa (*ISG15*) gene: sense primer, 5′-GAGAGG CAGCGAACTCATCT-3′; antisense primer, 5′-CTTCAG CTCTGACACCGACA-3′.[14] The *APOC1* gene: sense primer, 5′-TGAGGCTCTTCCTGTCGCTC-3′; antisense primer, 5′-CTGGGCCTTCCAAGACGA-3′,[15] the *NRIP2* gene: sense primer, 5′-GGAAGACCAGCAGGACAGAG-3′; antisense primer, 5′-TAGCTCCAACTGCTCCACCT-3′ and the *OMA1*: sense primer, 5′-TTGGATTGCTCTTTGTGGTG-3′; antisense primer, 5′-GGTATCGGGCATCTTTCTCA-3′ were used as validations for microarray analyses. The *ACBT* gene: sense primer, 5′-GCAAAGACCTGTACGCCAACA-3′; antisense primer, 5′-TGCATCCTGTCGGCAATG-3′ was used as an internal control.[16] Real-time monitoring of PCR was performed with the ABI 7500 Fast Real Time PCR system (Roche Applied Science) and Power SYBR Green PCR Master Mix (Roche Applied Science). Each assay was performed in triplicate.

Data analysis was performed using the $2^{-\Delta\Delta Ct}$ method described previously.[17]

Immunohistochemical analysis

Paraffin-embedded specimens from 70 patients with OSCC and 34 with ODL were used for Immunohistochemical (IHC) analysis. IHC staining was performed using the streptavidin–biotin immunoperoxidase technique with EnVision™+ Dual Link System-HRP (Dako, Glostrup, Denmark). Paraffin-embedded tissue sections (4 μm thick) were stained with rabbit polyclonal ISG15 antibody sc-50366 (Santa Cruz Biotechnology, Santa Cruz, CA) at 1:250 dilution according to the manufacturer's instruction. The intensity and percentage of positive staining of the target cells were determined by two oral surgeons blinded to the clinical parameters and used for quantitative scoring. Staining intensity was graded using four scores, with 0 representing no staining and 1, 2 and 3 indicating weak, moderate and strong staining, respectively. Scores were then multiplied by the percentage of positively stained cells to obtain the final protein expression score. The final expression scores were classified into four groups: negative staining (0; *i.e.* no stain), weak staining (10–70), moderate staining (80–170) and strong staining (>180).[18] Weak and moderate staining were defined as low expression, whereas strong staining was defined as high expression.

Statistical analysis

In the microarray studies, analysis of the gene expression data was performed using R statistical software version 2.12.1 (http://www.r-project.org). The Mann–Whitney *U* test was applied to determine the difference in the relative gene expression between normal tissues, ODLs and OSCCs. In the IHC assay, two-tailed Fisher's exact test was applied to determine the difference in the proportion of high expression between OSCCs and ODLs, and the results were compared with the clinicopathological data. DFS and OS were calculated by the Kaplan–Meier method and significance was determined by the log-rank test. The level of significance was set at $p < 0.05$. These statistical analyses were performed using SPSS 15.0J software (SPSS, Chicago, IL).

Results

Identification of differentially expressed genes in oral carcinogenesis

To identify genes associated with the development of oral cancer, we examined the gene expression profiles in normal, dysplastic and invasive cancer tissues obtained by LMD from 11 OSCC patients.

First, we investigated the differentially expressed genes between normal and dysplastic tissues, as well as between dysplastic and malignant tissues. We identified 890 genes that showed significant upregulation ($p < 0.05$ and FC > 1.2) in dysplasia compared with normal tissue. Likewise, 461 genes were upregulated in tumor compared with dysplastic tissues. It is interesting that the number of genes differentially upregulated in normal and dysplastic tissues was almost 2-fold greater than in dysplastic and tumor tissues. This suggests that the majority of genes upregulated during disease progression in oral cancer affect the sequence from the normal to the dysplastic state. Furthermore, consistent upregulation during disease progression toward dysplasia and invasive cancer was observed for the following ten genes: *ACTG2, APOC1, FCGR3A, ISG15, NRIP2, PZP, RAPGEF6, SLC29A3, STMN3* and *SYT10* (Fig. 1*b-1*). These genes are likely to be associated with both dysgenesis and tumorigenesis.

Next, we also investigated genes significantly downregulated during oral carcinogenesis ($p < 0.05$ and FC < 0.833 (1/1.2)). We identified 17 genes differentially downregulated between normal and dysplastic tissues, as well as 1,388 genes differentially downregulated between dysplastic and cancer tissue. Unlike genes upregulated during carcinogenesis, a high percentage of the differentially downregulated genes were found between the dysplastic and tumor states rather than between normal and dysplastic tissues. Consequently, the following five genes were differentially downregulated between both normal and dysplastic tissues and between dysplastic and tumor tissues: *FMO1, NUCB2, OMA1, TMPRSS1B* and NP_001006656.1 (*FAM149A*) (Fig. 1*b-2*). These genes showed consistent downregulation throughout the entire process of oral carcinogenesis (Table 1).

To investigate the expression patterns of genes consistently upregulated or downregulated during oral carcinogenesis, we performed hierarchical clustering analysis (Fig. 1*c*). Normal tissues and the majority of ODLs were classified into

Cancer Genetics

Table 1. Identified 15 candidate genes

Gene symbol	GeneBank accession no.	Function
Ten upregulated genes		
ACTG2	NM_001199893.1	Nucleotide binding
APOC1	NM_001645.3	Metabolic process
FCGR3A	NM_000569	Immune response
ISG15	NM_005101	Cell–cell signaling
NRIP2	NM_031474.2	Cell junction
PZP	NM_002864.2	Female pregnancy
RAPGEF6	NM_001164386.1	Signal transduction
SLC29A3	NM_001174098.1	Transmembrane transport
STMN3	NM_015894.2	Signal transduction
SYT10	NM_198992.3	Cell junction
Five downregulated genes		
FMO1	NM_002021.1	Metabolic process
FAM149A	NM_001006655.2	Unknown
NUCB2	NM_005013.2	DNA binding
OMA1	NM_145243.3	Proteolysis
TMPRSS11B	NM_182502	Proteplysis

the same cluster, whereas the invasive cancer tissues formed a cluster with a distinct pattern of gene expression. However, two dysplastic samples (D6 and D10) clustered with the malignant group. These samples had the histological appearance of severe dysplasia and were the most advanced of the premalignant lesions analyzed in the present study. In addition, these dysplastic tissues (D6 and D10) were assigned to adjacent nodes of the corresponding tumor tissue (T6 and T10, respectively), and gene expression profiling showed a close resemblance between them (D6 and T6, D10 and T10). This finding suggested that the gene expression profiles in some severe dysplastic tissues are similar to that of a malignant tumor.

Validation of microarray data by quantitative RT-PCR

To confirm these gene expression data identified by microarray analysis, total RNA isolated from different subset of normal, ODL and OSCC specimens was harvested for qRT-PCR. Three consistently upregulated genes with in the ten candidate genes, ISG15, APOC1, NRIP2 and, one consistently downregulated gene, OMA1 were chosen for confirmation. Consistently, with the microarray analysis, mRNA expression level of the ISG15, APOC1 and NRIP2 is significantly increased between normal tissues and ODLs and ODLs and OSCCs. On the contrary, OMA1 mRNA expression level was continuously decreased during the conversion both normal tissues to ODLs and also from ODLs to invasive OSCCs (Fig. 2). These findings indicate that the data obtained from the microarray analysis is reliable and that these 15 genes may be significant candidates, which contribute to the development of not only invasive cancer but also dysplastic lesions. Moreover, we focused on *ISG15* among these identified 15 genes, because recent microarray and proteomic studies have indicated that the expression of this gene is increased at the mRNA and protein levels in OSCC.[18,19]

IHC analyses

To validate protein expression of ISG15, IHC staining was performed on 70 OSCC and 34 ODL samples. As shown in Figures 3*a* and 3*b*, ISG15 was not found in adjacent normal epithelium; however, moderate to strong staining of ISG15 was detected in all tissue sections from OSCCs and 33 of 34 (97.1%) sections from ODLs. A strong immunochemical signal for ISG15 was detected predominantly in the cytoplasm, partially in the nucleus of the OSCC and ODL cells. Among the 70 tissue sections from OSCCs, 37 (52.9%) exhibited high expression and 33 (47.1%) showed low expression levels. By contrast, among 34 sections from ODLs, seven (20.6%) showed high expression, 26 (76.5%) exhibited low expression and one (2.9%) showed no staining. ISG15 high expression in OSCCs was significantly more common than in ODLs ($p = 0.003$) (Fig. 3*c*). IHC analysis clearly demonstrated that ISG15 protein expression was specifically detected in ODLs and OSCCs, indicating that *ISG15* is likely to be associated with both dysgenesis and tumorigenesis.

Clinicopathological significance of ISG15 protein expression in OSCC

The correlation between ISG15 protein expression and clinicopathological features of the 70 OSCCs are summarized in Table 2. There were no significant associations between ISG15 protein expression level and age, gender, disease stage, cellular differentiation, mode of invasion, nodal status or recurrence. By contrast, the incidence of mortality was significantly higher ($p = 0.027$) in the high-expression group (10 of 38; 26.3%) than in the low expression group (2 of 33; 6.1%).

Relationship between ISG15 protein expression and survival

There was no recurrence in 23 of 37 patients (62.2%) with ISG15 high expression and in 24 of 33 patients (72.7%) with ISG15 low expression. In patients with ISG15 high expression, the DFS curve was lower than that of the patients with ISG15 low expression, although this failed to reach statistical significance ($p = 0.281$) (Fig. 4*a*). Conversely, 27 of 37 patients (73.0%) with ISG15 high expression and 31 of 33 patients (93.9%) with ISG15 low expression remained alive. Kaplan–Meier survival curves clearly demonstrated the adverse impact of ISG15 high expression on OS ($p = 0.019$) (Fig. 4).

Discussion

In the present study, we selected 890 and 461 genes that showed significant increase in expression in ODLs compared with the corresponding normal tissues and in invasive

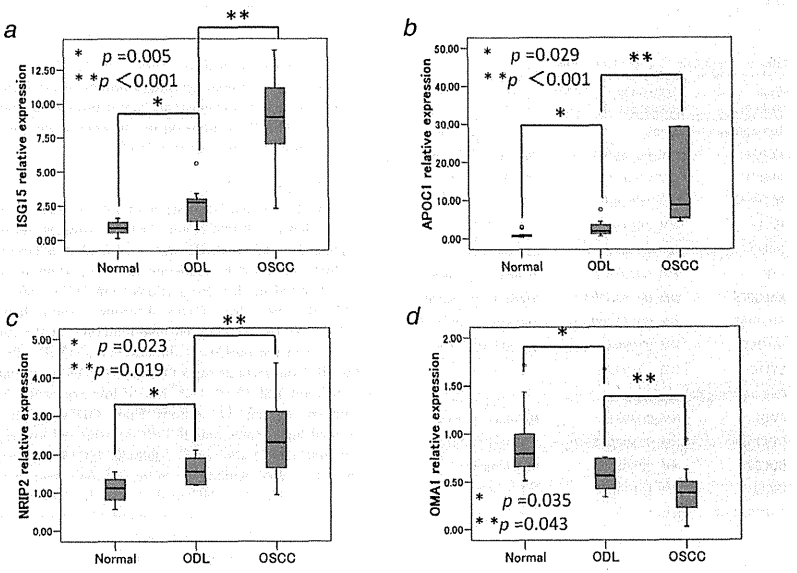

Figure 2. (*a*) *ISG15*, (*b*) *APOC1*, (*c*) *NRIP2* and (*d*) *OMA1* mRNA expression in the normal tissues from OSCC, ODLs and OSCCs by qRT-PCR.

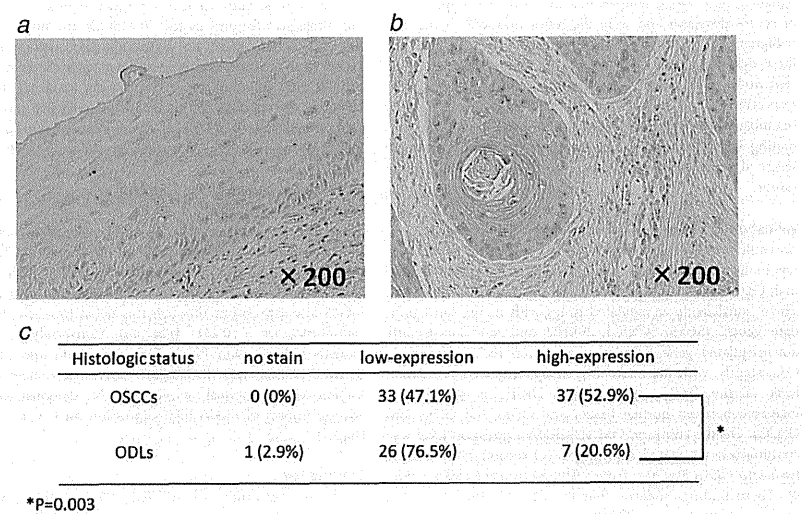

Figure 3. Immunohistochemical analysis of ISG15 in OSCC and normal tissue. Immunohistochemical analysis using anti-ISG15 polyclonal antibody confirmed the elevated expression of this protein in OSCC cells compared with in normal epithelium. (*a*) Normal epithelium; (*b*) high expression of OSCC and (*c*) immunohistochemical staining of ISG15 protein expression in the OSCCs and ODLs.

cancers compared the corresponding ODLs, respectively. In addition, we also identified 17 significantly differentially downregulated genes between normal tissue and ODLs, as well as 1,388 genes differentially downregulated between dysplastic and cancer tissues. These findings suggest that the majority of genes upregulated during disease progression in oral cancer affect the sequence from the normal to the dysplastic state. On the other hand, a high percentage of genes were downregulated during the progression from ODLs to invasive cancer. However, Ha *et al.* have investigated gene expression profile in seven cases of HNSCC compared with eight premalignant lesions and 11 normal matched and unmatched controls using expression microarray analysis. In contrast to the present results, they demonstrated that a greater proportion of transcriptional changes including both upregulation and downregulation occur during the transition from normal to premalignant mucosa than in the transition from premalignant to malignant lesions. Based on these observations, they concluded that premalignant lesions may possess many of the alterations found in cancer before the development of a malignant phenotype.[7] A direct comparison between the study of Ha *et al.* and the present study is difficult because (*i*) they used bulk samples, whereas we used microdissected samples from identical OSCCs (to remove stromal cells); (*ii*) they assayed samples with gene expression arrays containing >12,000 genes, whereas we examined 35,035 probes on the Human V4.0 OpArray and (*iii*) the sample sites were different (general HNSCCs *vs.* SCCs specifically of the oral cavity). Therefore, this issue is still a matter of controversy and further investigations are required.

In this study, we identified 15 overexpressed or underexpressed genes that may play an important role in the oral carcinogenic pathway. Then, we focused on one of these genes, *ISG15*. Several microarray analyses of human tumors have revealed enhanced expression of *ISG15* in pancreatic adenocarcinoma, endometrial cancer and bladder cancer, compared with respective normal tissues.[20,21] In addition, recent microarray and proteomics studies have demonstrated that mRNA and protein overexpression of this gene is frequently detected in OSCCs, suggesting that *ISG15* may contribute to the development of this malignancy.[18,19] These findings support the need for further investigation. Thus, in the present study, we investigate for the first time ISG15 expression at both mRNA and protein levels in ODLs and invasive OSCCs to confirm the contribution of this gene to oral carcinogenesis and also to examine the association between ISG15 expression status and both clinicopathological parameters and patient survival. As a result, we clearly demonstrated the ISG15 mRNA and protein expression level continuously increase during the conversion both from normal tissues to ODLs and also from ODLs to invasive OSCCs. This finding indicates that ISG15 may contribute to the development of not only ODLs but also OSCCs. Furthermore, we found a significant correlation between high expression of ISG15 and unfavorable prognosis ($p = 0.027$). In addition, Kaplan–Meier analysis showed that the OS period in patients whose tumors exhibited high ISG15 expression was significantly shorter than in patients with low-expression tumors ($p = 0.019$), suggesting a critical role of ISG15 in the acquisition of the malignant phenotype of OSCC. The question arises as to why tumors with high expression of ISG15 have an aggressive phenotype. ISG15 expression was stimulated by type I interferon pathway (*i.e.* IFN-β), and IFN-β treatment significantly enhanced the expression of *ISG15* as well as the migration ability of the OSCC cell line.[18] Moreover, very recently, the ISG15 pathway could disrupt cytoskeletal architecture and promotes motility in human breast cancer cells and consequently enhanced metastatic ability of cancer cells. In addition, this protein inhibits targeted degradation of proteins involved in cell motility, invasion and metastasis.[22] Thus, one possible answer is that tumors with abundant *ISG15* expression may have a high migration and invasion ability. A second possibility is an insufficient response to chemotherapy in this subgroup of patients with high-expression tumors.[18] It is clear that deregulated *ISG15* expression has been observed in response to various chemotherapeutic agents, such as paclitaxel in the treatment of ovarian carcinomas and 5-fluorouracil therapy for esophageal cancers.[23,24] However, the putative function of *ISG15* in oral tumorigenesis and in chemotherapeutic response requires further analysis in prospective studies.

Oral epithelial dysplasia is a potentially precancerous lesion diagnosed histopathologically. While histological grade is currently the best predictor of progression, it is impossible to predict accurately which lesions will progress to invasive cancer. The more accurate markers predicting the progression would enable better diagnosis of these lesions and more appropriate selection of aggressive treatment and closer follow-up.[25] Such biomarkers should be proteins or genes that can be differentially expressed in cancer, precancer and normal tissue. Thus, we aimed to identify those genes with progressively increased or decreased expression during oral carcinogenesis by means of LMD and microarray analyses. We determined 15 genes and focused on one of these, *ISG15*. Subsequently, we confirmed that the mRNA expression level of this gene is significantly different in normal tissue and precancerous lesion, as well as in precancerous lesions and invasive cancer. Moreover, IHC analyses clearly demonstrated that although ISG15 protein expression was not found in normal epithelium, moderate to strong staining of this gene was detected in almost all ODLs and OSCCs, and high expression of ISG15 in invasive cancers was significantly more common than in precancerous lesions ($p = 0.003$), suggesting that the protein expression level of this gene is enhanced according to the degree of malignant transformation. These observations indicated that *ISG15* may discriminate between ODLs with and without malignant potential and may be a potential molecular marker that can predict disease progression to invasive OSCC. However, to determine the sensitivity, predictability and reproducibility of *ISG15* to predict the progression to invasive cancer, a larger multicenter study with longitudinal design is required.

In conclusion, this microarray study identified 15 overexpressed or underexpressed genes that may contribute to the development of OSCC. mRNA expression of one of the extracted genes, *ISG15*, was significantly different between both normal tissues and ODLs and ODLs and OSCCs. In addition, the protein expression level was enhanced according to the degree of malignant transformation, and high expression of this gene was significantly correlated with poor prognosis of patients with OSCC. These findings indicate that *ISG15* plays an important role in the initiation and progression of oral tumorigenesis and may be a potential prognostic marker with the ability to predict disease progression to invasive OSCC. Further studies are needed to evaluate the prognostic and diagnostic potential of *ISG15* and to address the potential role of this gene in oral carcinogenesis.

Table 2. Clinicopathological parameters of 70 OSCCs and correlation with ISG15 protein expression

	Total number	ISG15 protein expression: Low expression	ISG15 protein expression: High expression	p^1
Age (years)				
<60	35	18	17	
≥60	35	15	20	NS
Gender				
Male	52	24	28	
Female	18	9	9	NS
Disease stage				
I, II	48	21	27	
III, IV	22	12	10	NS
Cellular differentiation				
Well to moderate	57	27	30	
Poor	13	6	7	NS
Mode of invasion				
1–3	40	21	19	
4C–4D	26	9	17	NS
Nodal status[2]				
No metastasis	51	22	29	
Metastasis	18	10	8	NS
Recurrence				
Negative	47	24	23	
Positive	23	9	14	NS
Survival				
Alive	58	31	27	
Dead	12	2	10	0.027

[1]By two-tailed Fisher exact test. [2]Histopathlogic diagnosis.
Abbreviation: NS, not significant.

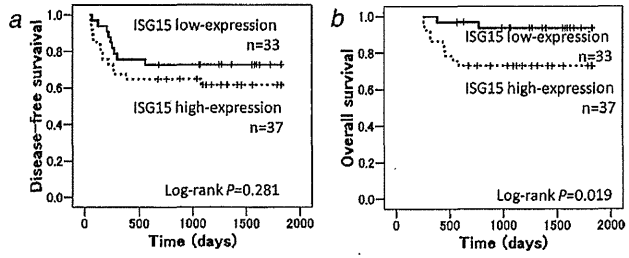

Figure 4. Kaplan–Meier plots for (*a*) disease-free survival according to ISG15 protein status and (*b*) overall survival according to ISG15 protein status.

Acknowledgements

The authors express our appreciation to hospital staffs of diagnostic oral pathology for their technical assistance and advice.

References

1. Parkin DM, Bray F, Ferlay J, et al. Global cancer statistics, 2002. *CA Cancer J Clin* 2005; 55:74–108.
2. Méndez E, Cheng C, Farwell DG, et al. Transcriptional expression profiles of oral squamous cell carcinomas. *Cancer* 2002;95: 1482–94.
3. van der Waal I. Potentially malignant disorders of the oral and oropharyngeal mucosa: present concepts of management. *Oral Oncol* 2010;46: 423–5.
4. Kramer IR, Lucas RB, Pindborg JJ, et al. Definition of leukoplakia and related lesions: an aid to studies on oral precancer. *Oral Surg Oral Med Oral Pathol* 1978;46:518–39.
5. Amagasa T, Yamashiro M, Uzawa N. Oral premalignant lesions: from a clinical perspective. *Int J Clin Oncol* 2011;16:5–14.
6. Nankivell P, Mehanna H. Oral dysplasia: biomarkers, treatment, and follow-up. *Curr Oncol Rep* 2011;13:145–52.
7. Ha PK, Benoit NE, Yochem R, et al. A transcriptional progression model for head and neck cancer. *Clin Cancer Res* 2003;9: 3058–64.
8. Califano J, van der Riet P, Westra W, et al. Genetic progression model for head and neck

Cancer Genetics

cancer: implications for field cancerization. *Cancer Res* 1996;56:2488–92.
9. Irié T, Aida T, Tachikawa T. Gene expression profiling of oral squamous cell carcinoma using laser microdissection and cDNA microarray. *Med Electron Microsc* 2004;37:89–96.
10. Choi P, Chen C. Genetic expression profiles and biologic pathway alternation in head and neck squamous cell carcinoma. *Cancer* 2005;104: 1113–28.
11. Simone NL, Bonner RF, Gillespie JW, et al. Laser-capture microdissection: opening the microscopic frontier to molecular analysis. *Trends Genet* 1998;14:272–6.
12. Jakobsson PA, Eneroth CM, Killander D, et al. Histologic classification and grading of malignancy in carcinoma of the larynx. *Acta Radiol Ther Phys Biol* 1973;12:1–8.
13. Yamamoto E, Kohama G, Sunakawa H, et al. Mode of invasion, bleomycin sensitivity, and clinical course in squamous cell carcinoma of the oral cavity. *Cancer* 1983;51: 2175–80.
14. Bektas N, Noetzel E, Veeck J, et al. The ubiquitin-like molecule interferon-stimulated gene 15 (ISG15) is a potential prognostic marker in human breast cancer. *Breast Cancer Res* 2008;10: R58.
15. Oue N, Hamai Y, Mitani Y, et al. Gene expression profile of gastric carcinoma: identification of genes and tags potentially involved in invasion, metastasis, and carcinogenesis by serial analysis of gene expression. *Cancer Res* 2004;64:2397–405.
16. Begum A, Imoto I, Kozaki K, et al. Identification of PAK4 as a putative target gene for amplification within 19q13.12-q13.2 in oral squamous-cell carcinoma. *Cancer Sci* 2009;100: 1908–16.
17. Livak KJ, Schmittgen TD. Analysis of relative gene expression data using real-time quantitative PCR and the 2(-Delta Delta C(T)) Method. *Methods* 2001;25:402–8.
18. Chi LM, Lee CW, Chang KP, et al. Enhanced interferon signaling pathway in oral cancer revealed by quantitative proteome analysis of microdissected specimens using 16O/18O labeling and integrated two-dimensional LC-ESI-MALDI tandem MS. *Mol Cell Proteomics* 2009;8:1453–74.
19. Ye H, Yu T, Temam S, et al. Transcriptomic dissection of tongue squamous cell carcinoma. *BMC Genomics* 2008;9:69.
20. Andersen JB, Aaboe M, Borden EC, et al. Stage-associated overexpression of the ubiquitin-like protein, ISG15, in bladder cancer. *Br J Cancer* 2006;94: 1465–71.
21. Desai SD, Haas AL, Wood LM, et al. Elevated expression of ISG15 in tumor cells interferes with the ubiquitin/26S proteasome pathway. *Cancer Res* 2006;66:921–8.
22. Desai SD, Reed RE, Burks J, et al. ISG15 disrupts cytoskeletal architecture and promotes motility in human breast cancer cells. *Exp Biol Med* 2012; 237:38–49.
23. Bani MR, Nicoletti MI, Alkharouf NW, et al. Gene expression correlating with response to paclitaxel in ovarian carcinoma xenografts. *Mol Cancer Ther* 2004;3:111–21.
24. Matsumura Y, Yashiro M, Ohira M, et al. 5-Fluorouracil up-regulates interferon pathway gene expression in esophageal cancer cells. *Anticancer Res* 2005;25: 3271–8.
25. Smith J, Rattay T, McConkey C, et al. Biomarkers in dysplasia of the oral cavity: a systematic review. *Oral Oncol* 2009; 45:647–53.

IJC
International Journal of Cancer

Identification of NUCKS1 as a colorectal cancer prognostic marker through integrated expression and copy number analysis

Akifumi Kikuchi[1], Toshiaki Ishikawa[2], Kaoru Mogushi[3], Megumi Ishiguro[1], Satoru Iida[1], Hiroshi Mizushima[4], Hiroyuki Uetake[2], Hiroshi Tanaka[3] and Kenichi Sugihara[1]

[1] Department of Surgical Oncology, Graduate School, Tokyo Medical and Dental University, 1-5-45 Yushima, Bunkyo-ku, Tokyo, Japan
[2] Translational Oncology, Graduate School, Tokyo Medical and Dental University, 1-5-45 Yushima, Bunkyo-ku, Tokyo, Japan
[3] Department of Systems Biology, Graduate School of Biochemical Science, Tokyo Medical and Dental University, 1-5-45 Yushima, Bunkyo-ku, Tokyo, Japan
[4] Department of Medical Omics Informatics, School of Biochemical Science, Tokyo Medical and Dental University, 1-5-45 Yushima, Bunkyo-ku, Tokyo, Japan

We identified a novel prognostic biomarker for the distant metastasis of colorectal cancer (CRC) using comprehensive combined copy number and gene expression analyses. Expression of mRNA in CRC tissue was profiled in 115 patients using an Affymetrix Gene Chip, and copy number profiles were generated for 122 patients using an Affymetrix 250K Sty array. Genes showing both upregulated expression and copy number gains in cases involving distant CRC metastasis were extracted as candidate biomarkers. Expression of the candidate gene mRNA was validated in 86 patients using quantitative reverse transcription polymerase chain reaction assays. Expression of the protein encoded by the candidate gene was assessed using immunohistochemical staining of tissue from 269 patients. The relationship between protein expression and clinicopathologic features was also examined. Following combined copy number and gene expression analyses, three genes linked to distant metastasis of CRC were extracted as candidate biomarkers. The expression of NUCKS1, reportedly overexpressed in several cancers other than CRC, was significantly higher in CRC tissue than in normal tissue. Overexpression of the NUCKS1 protein in CRC cells was found to be associated with significantly worse overall survival and relapse-free survival, indicating that NUCKS1 is an independent risk factor for CRC recurrence. The overexpression of NUCKS1 in cancer cells could be used as a CRC prognostic marker and might also be a target for treatment of this disease.

Colorectal cancer (CRC) is now the third most prevalent cancer and the second leading cause of cancer-related mortality worldwide.[1] In Japan, the incidence of CRC has doubled over the past 20 years such that CRC is now the second most deadly neoplastic disease.[2,3]

Surgery is still the most effective treatment for CRC. Among those patients that undergo curative surgery, some develop local recurrence or distant metastases that lead to shorter survival times.[4] Distant metastasis has a critical influence on the prognosis of CRC. Clinicopathologic indicators such as the tumor node metastasis (TNM) classification system of the International Union Against Cancer (UICC) remain the standard for prognosis and provide the basis for therapeutic decision making. However, clinicopathologic indicators alone do not enable clinicians to make precise prognoses for individual CRC patients.[5] In order to develop personalized therapy regimens, it is therefore critical that researchers identify novel genes involved in distant metastasis that can serve as predictive biomarkers.[6] A particularly powerful tool for identifying potential biomarker genes for use in cancer prognosis is the microarray.[7–9] It is now possible with microarray analysis to investigate several thousand cancer-related or cancer-specific genes at once.

Chromosomal structural alterations play an important role in cancer development. In CRC, copy number aberrations (CNAs), including gains on chromosomes 7, 8, 13 and 20, and losses on chromosomes 1p, 8p, 17p and 18, are also frequently observed.[10–13] Some of the CNAs are related to the metastasis of CRC and can thus be used in prognosis. Recently, single nucleotide polymorphism microarray (SNP array) analysis has become a useful tool for examining CNAs, permitting highly accurate exploration of thousands of genetic markers in a single study.[14]

Studies of the relationship between chromosomal aberrations and gene expression in cancers, including CRC, have shown that CNAs directly influence gene expression.[15–19] Several groups have thus suggested that integrating gene expression analysis with genomic profiling represents an efficient approach to discover cancer-related genes.[20–22] Genes which show a strong positive correlation between expression and copy number may play an important role in cancer progression. Thus, in this study, we integrated gene expression and copy number analyses to identify novel genes associated with the distant metastasis of CRC. We focused on those genes that are overexpressed and have an amplified copy number in cases of distant metastasis because this indicates that they have a potential to serve as useful therapeutic targets or clinical biomarkers.

Using the aforementioned comprehensive analysis, we identified *NUCKS1* (nuclear, casein kinase and cyclin-dependent kinase substrate 1) as a gene involved in the distant metastasis of CRC. It has been suggested that NUCKS1 plays an important role in cell cycle progression,[23] and overexpression of NUCKS1 has been reported in several cancers, although not in CRC.[24–28] Ours is the first study to demonstrate the clinicopathologic significance of NUCKS1 expression in CRC, using integrated copy number and gene expression analyses of clinical tissue samples.

Key words: colorectal cancer, biomarker, gene expression analysis, DNA copy number analysis, microarray
DOI: 10.1002/ijc.27911
History: Received 30 Mar 2012; Accepted 24 Sep 2012; Online 15 Oct 2012
Correspondence to: Akifumi Kikuchi, Department of Surgical Oncology, Graduate School, Tokyo Medical and Dental University, 1-5-45 Yushima, Bunkyo-ku, Tokyo 113-8519, Japan, Tel.: +81-3-5803-5261, Fax: +81-3-5803-0139, E-mail: akifumi_kikuchi@tmhp.jp

What's new?
The integration of gene expression analysis and genomic profiling represents an efficient approach to the discovery of cancer-related genes. Here, through a combination of gene expression and copy number analysis, *NUCKS1* was identified as a candidate gene involved in the distant metastasis of colorectal cancer. The association of NUCKS1 protein overexpression with poor overall survival in colorectal cancer suggests that NUCKS1 may be a prognostic marker for the disease.

Material and Methods

Patients

Primary tumors from 392 patients who underwent curative surgery for CRC between 2002 and 2007 at the Tokyo Medical and Dental University Hospital (Tokyo, Japan) were used in this study. Written informed consent was obtained from all patients, and the study was approved by the Institutional Review Board. Clinical data were obtained from the medical records of each patient, and histopathological evaluations were assessed by reference to the criteria of the TNM-system of the UICC, 6th edition. A total of 123 patients were assigned to the comprehensive analyses for extraction of candidate genes. Of these patients, 114 were assigned to both the gene expression and the CNA studies, 8 patients were assigned only to the CNA study, and 1 patient was assigned only to the gene expression study. Thus, a total of 122 patients were assigned to the CNA study, including 18 patients with Stage I, 42 patients with Stage II, 37 patients with Stage III and 25 patients with Stage IV disease. The median follow-up time for these patients was 24 months (range = 1–40 months). A total of 115 patients were assigned to the gene expression study, including 16 patients with Stage I, 41 patients with Stage II, 35 patients with Stage III and 23 patients with Stage IV disease. The median follow-up time for these patients was 28 months (range = 1–40 months).

Quantitative reverse transcription polymerase chain reaction (RT-PCR) assays were performed for validation using samples from 86 patients with CRC, including 9 patients with Stage I, 26 patients with Stage II, 33 patients with Stage III and 18 patients with Stage IV disease. The median follow-up time for these patients was 48 months (range = 1–61 months). Moreover, 269 patients, including patients subjected to RT-PCR validation, were assigned to an immunohistochemical study. The immunohistochemical study included 48 patients with Stage I, 84 patients with Stage II, 87 patients with Stage III and 50 patients with Stage IV disease. The median follow-up time for these patients was 46 months (range = 1–95 months). It should be noted that the 269 patients assigned to these validation studies were not the same patients enrolled in the comprehensive analyses.

DNA extraction

After resection, cancer tissues were immediately embedded in Tissue-Tek OCT compound medium (Sakura Finetek Japan, Tokyo, Japan). Serial frozen sections of 9-μm in thickness were mounted onto a 90 FOIL-SL25 foil-coated glass slide (Leica Microsystems, Wetzlar, Germany). Laser capture microdissection (LCM) was performed using an Application Solutions LCM System (Leica Microsystems). Tumor DNA was extracted and purified using a QIAamp DNA micro kit (Qiagen, Hilden, Germany) according to the manufacturer's instructions. Non-neoplastic tissues were homogenized in microtubes, and DNA was extracted and purified from these tissues using a QIAamp DNA mini kit (Qiagen) according to the manufacturer's instructions.

CNA analysis

Copy number analysis was performed using a GeneChip® Human Mapping 250K Sty array (Affymetrix, Santa Clara, CA) in strict adherence to the assay manual. Genomic DNA was digested using the enzyme Sty I, and adaptor Sty I was used prior to the PCR reaction. Amplicons were fragmented after purification and then labeled. After hybridization, the microarrays were transferred to a totally automated GeneChip® Fluidics Station 450 (Affymetrix) for the washing and staining steps. After fluorescence staining, microarray images were scanned using a GeneChip® Scanner 3000 7G (Affymetrix). The microarray data from the scanner were used for copy number analysis with the Chromosome Copy Number Analysis Tool (Affymetrix). Copy number data sets were submitted to Gene Expression Omnibus (http://www/ncbi.nlm.nih.gov/geo/, accession number GSE27910). Data were analyzed using R statistical software (version 2.12.1; http://www.r-project.org/).

RNA extraction

Cancer cells were microdissected using LCM. Total RNA was extracted from cancer cells and purified using an RNeasy

micro kit (Qiagen) with on-column DNase digestion, according to the manufacturer's instructions. Total RNA collected from bulk samples of cancer tissues and adjacent non-neoplastic tissues was extracted and purified using an RNeasy mini kit (Qiagen) with on-column DNase digestion, according to the manufacturer's instructions. The integrity of the total RNA was assessed using an Agilent 2100 BioAnalyzer (Agilent Technologies, Palo Alto, CA). Samples with an RNA integrity number greater than 5.0 were used for the rest of the experiments.

Gene expression analysis

Complementary RNA was prepared from total RNA extracted from laser capture microdissected cancer cells collected from 115 patients using two-cycle target labeling and a control reagents kit (Affymetrix). The experiment was performed using the GeneChip® Human Genome U133 Plus 2.0 Array (Affymetrix), according to the manufacturer's instructions. The gene expression data sets were submitted to Gene Expression Omnibus (http://www/ncbi.nlm.nih.gov/geo/, accession number GSE27854). Statistical analyses of microarray data were normalized using the robust multi-array average method with R statistical software (version 2.12.1; http://www.r-project.org/) together with the BioConductor package (http://www.bioconductor.org/).

Extraction of candidate genes

We defined patients with synchronous or metachronous distant metastases as the metastatic group, and patients without any distant metastases as the non-metastatic group. The metastasis which was recognized at the surgical operation of the primary tumor was synchronous metastasis. The metastasis which appeared after surgery was metachronous metastasis. The CNA data and the gene expression data were analyzed and compared between the two groups to identify genes involved in the distant metastasis of CRC.

Data regarding genes which showed a copy number gain in the metastatic group were extracted using Fisher's exact test ($p < 0.01$). Data regarding genes that were significantly upregulated in the metastatic group were extracted using the Wilcoxon exact rank sum test ($p < 0.01$). Among the genes that were common to both groups, those that were overexpressed (fold change > 1.3) in the metastatic group were selected as candidates for further analysis.

Quantitative RT-PCR

Total RNA collected from bulk samples of cancer tissues and adjacent non-neoplastic tissues was reverse-transcribed into cDNA using a High Capacity cDNA Reverse Transcription Kit (Applied Biosytems, Foster City, CA) according to the manufacturer's instructions. A TaqMan® gene expression assay (Applied Biosystems; NUCKS1; Hs00224144_m1, β-actin; Hs99999903_m1) was used to investigate the expression of *NUCKS1*, and β-actin was used as an internal control. The PCR reaction was carried out using TaqMan® Universal PCR Master Mix (Applied Biosystems). The thermal cycling conditions were as follows: 50°C for 2 min, 95°C for 10 min and 40 cycles of denaturation at 95°C for 15 sec and annealing at 60°C for 1 min. All calculated concentrations of target genes were normalized by the amount of the endogenous reference using the comparative Ct method for relative quantification with Relative Quantification Study Software (7300 Sequence Detection System version 1.2.1, Applied Biosystems).

Immunohistochemistry

A streptavidin-biotin method was used for immunostaining NUCKS1. Tissue sections were obtained from formalin-fixed paraffin-embedded tissue blocks from each patient. After deparaffinization in xylene and rehydration through a series of incubations in decreasing concentrations of ethanol, antigen was retrieved from the tissues by autoclaving them at 121°C for 15 min in pH 6.0 citrate buffer. The slides were then incubated in a solution of 3% hydrogen peroxide in 100% methanol for 15 min at room temperature in order to quench endogenous peroxidase activity. Nonspecific binding was blocked by treating the tissues with 10% normal goat serum (Nichirei Bioscience, Tokyo, Japan) for 10 min. Thereafter, the slides were incubated with a rabbit polyclonal antibody against NUCKS1 at a 1:900 dilution (ab84710, Abcam, Cambridge, UK) for 90 min at room temperature. Next, the slides were incubated with biotinylated anti-rabbit IgG (Nichirei Bioscience) for 10 min at room temperature, followed by peroxidase conjugated streptavidin (Nichirei Bioscience) for 5 min at room temperature. Color development was carried out with 0.02% 3,3′-diaminobenzidine tetrahydrochloride (Nichirei Bioscience). The slides were counterstained with 1% Mayer's hematoxylin, after which they were dehydrated using an increasing alcohol concentration series, immersed in xylene, and finally coverslipped.

All sections were scored by two investigators. The staining intensity was scored as 0 (negative), 1 (weak), 2 (moderate) or 3 (strong). The extent of staining was scored as 1 (1–10% of the tumor cells stained), 2 (11–40%), 3 (41–70%) or 4 (71%–100%). The sum of the intensity and extent scores, potentially ranging from 1 to 7, was used as the final staining score.

Statistical analysis of NUCKS1 expression

Statistical analyses of NUCKS1 expression were carried out using SPSS (version 17.0, SPSS Inc, Chicago, IL) software for Windows. To estimate the significance of differences between groups, Wilcoxon signed-rank, Mann–Whitney U and χ^2 tests were used where appropriate. Survival curves were estimated using the Kaplan–Meier method, and curves were compared using the log-rank test. Survival times were determined from the date of surgery. Prognostic factors were examined with univariate and multivariate analyses using the Cox proportional hazards model. A p value < 0.05 was considered statistically significant.

Cancer Genetics

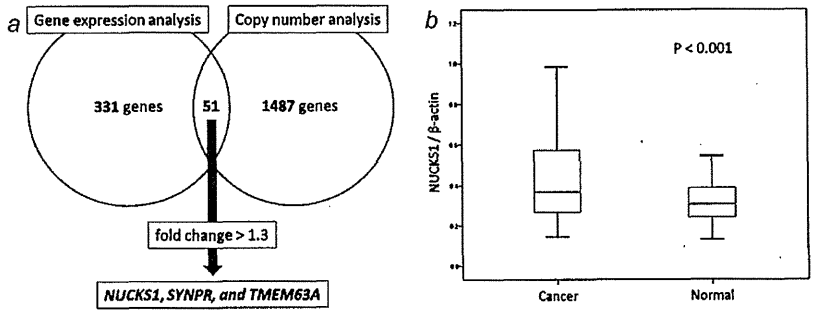

Figure 1. (*a*) A total of 331 genes were extracted from the gene expression analysis, and 1,487 genes were extracted from the CNA analysis. Among the 51 genes extracted from both analyses, three genes with a fold change in expression > 1.3 were selected as candidates for further analysis. (*b*) RT-PCR analysis showed that NUCKS1 mRNA expression is higher in cancer tissue than in adjacent non-neoplastic tissue ($p < 0.001$).

Results

Gene expression and copy number analyses

The copy number of 1,487 genes and the expression of 331 genes were elevated in tissues of patients with CRC with distant metastasis. Among the 51 genes with both elevated copy number and expression, the expression of *NUCKS1*, *SYNPR* and *TMEM63A* was upregulated with a fold change > 1.3 (Fig. 1*a*). Of these three genes, only *NUCKS1* has been shown to be associated with cancer. Overexpression of *NUCKS1* has been reported to occur in several cancers, although it has not been reported in CRC.[24–28] Thus, we focused on *NUCKS1* in the subsequent analyses.

NUCKS1 mRNA expression

Quantitative RT-PCR analysis of CRC tissue from 86 patients showed that expression of *NUCKS1* mRNA is significantly higher in cancerous tissue than in neighboring non-neoplastic tissue ($p < 0.001$; Fig. 1*b*). There was no significant difference in the level of *NUCKS1* mRNA expression between the metastatic group ($n = 31$) and the non-metastatic group ($n = 55$) ($p = 0.676$; data not shown).

Expression of NUCKS1 protein

The localization of the NUCKS1 protein was investigated using cancer tissue from the same 86 patients with CRC that were used for RT-PCR analysis. Immunohistochemical staining indicated that NUCKS1 is localized in the nucleus of CRC cells. Staining for NUCKS1 in normal epithelial cells adjacent to the cancer cells was negative or weak, and was also weak in the marginal tissue of the tumor. Strong staining tended to be located at the invasive tumor front (Fig. 2*a*). Thus, we concluded that the staining level at the invasive tumor front is important and examined NUCKS1 expression in this area in CRC tissue samples from 269 patients. As shown in Figure 2*b*, strong NUCKS1 staining was observed in lymphocytes and macrophages in the stroma.

Relationship between expression of NUCKS1 and clinicopathologic features

For statistical evaluation purposes, the 269 samples that underwent immunohistochemical analysis were divided into two groups: a high-expression group (final staining score of ≥ 6, $n = 107$) and a low-expression group (final staining score of ≤ 5, $n = 162$). The scoring cutoff point was determined using receiver operating characteristic (ROC) curve analysis. The ROC curve was generated to show the relationship between the sensitivity and false-positive rate at different NUCKS1 distant metastasis staining score cutoff points.

The correlation between NUCKS1 expression and various clinicopathologic factors is shown in Table 1. Tumor depth (T3/T4; $p = 0.038$), lymphatic invasion ($p < 0.001$), venous invasion ($p = 0.027$), lymph node metastasis ($p < 0.001$), carcinoembryonic antigen (CEA) level (5.0 ng/ml or higher; $p < 0.001$) and TNM stage (Stage IV; $p = 0.001$) are significantly associated with overexpression of NUCKS1. The overall survival (OS) rate was significantly lower ($p < 0.001$) in the high-expression group than in the low-expression group (Fig. 3*a*). Univariate analysis indicated that histology ($p < 0.001$), tumor depth ($p < 0.001$), lymphatic invasion ($p < 0.001$), venous invasion ($p = 0.017$), lymph node metastasis ($p < 0.001$), CEA level ($p < 0.001$), stage ($p < 0.001$) and NUCKS1 expression ($p < 0.001$) are significantly associated with OS (data not shown). Multivariate analysis indicated that overexpression of NUCKS1 is a significant prognostic factor of OS for patients with CRC ($p = 0.024$; relative risk (RR) $= 0.604$; 95% confidence interval $= 0.389$–0.937) (data not shown).

The correlation between NUCKS1 expression and various clinicopathologic factors in 218 patients with Stages I, II and

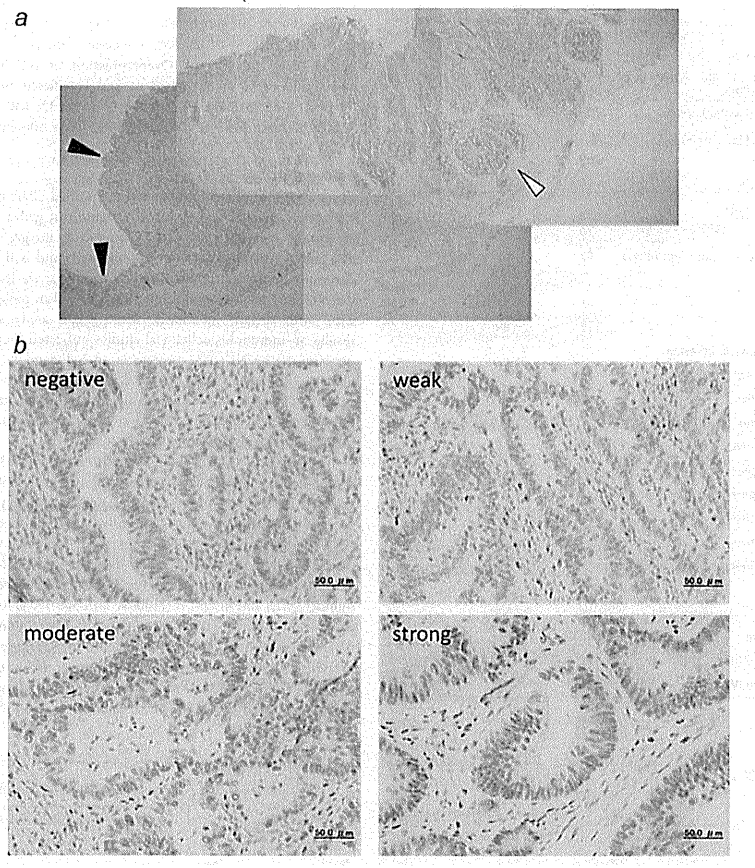

Figure 2. Representative images showing immunostaining of colorectal carcinoma tissue for NUCKS1. (*a*) NUCKS1-positive staining tended to be stronger along the invasive tumor front (white arrow) than in normal epithelial tissue and the marginal tissue of the tumor (black arrows) (magnification 40×). (*b*) Representative images of the invasive tumor front showing negative, weak, moderate and strong staining (magnification 400×).

III CRC is shown in Table 2. Lymphatic invasion (p = 0.001), venous invasion (p = 0.013), lymph node metastasis (p = 0.001) and CEA level (5.0 ng/ml or higher; p = 0.003) are significantly associated with overexpression of NUCKS1. The relapse-free survival (RFS) rate was significantly lower (p < 0.001) in the high-expression group than in the low-expression group (Fig. 3*b*). Univariate analysis indicated that histology (p = 0.007), tumor depth (p < 0.001), lymphatic invasion (p < 0.001), venous invasion (p = 0.015), lymph node metastasis (p < 0.001), CEA level (p < 0.001) and NUCKS1 expression (p < 0.001) are significantly associated with RFS (Table 3). Multivariate analysis indicated that NUCKS1 overexpression is an independent and significant prognostic factor of RFS for patients with Stages I, II and III CRC (p < 0.001; RR = 0.286; 95% confidence interval = 0.158–0.516) (Table 3). Moreover, multivariate analysis

Table 1. Relationship between clinicopathologic variables and NUCKS1 expression in patients with stage I-IV colorectal cancer

Variables	NUCKS1 expression Low (n = 162)	High (n = 107)	p
Age (Median), years	20–92 (66)	41–90 (72)	0.567
Gender			
Male	103	68	0.996
Female	59	39	
Histology			
Well	70	37	0.175
Moderate, poor and others	92	69	
Depth			
T1/T2	45	18	0.038
T3/T4	117	89	
Lymphatic invasion			
Negative	53	13	<0.001
Positive	108	94	
Venous invasion			
Negative	27	8	0.027
Positive	134	99	
Lymph node metastasis			
Negative	99	40	<0.001
Positive	63	67	
Carcinoembryonic antigen (ng/ml)			
<5	109	48	<0.001
≥5	46	56	
Stage			
Stage I-III	142	77	0.001
Stage IV	20	30	

indicated that NUCKS1 overexpression is an independent and significant prognostic factor of RFS in Stage II patients (p = 0.002; RR = 0.165; 95% confidence interval = 0.053–0.520) (data not shown). Overexpression of NUCKS1 was also found to be an independent and significant prognostic factor of RFS in Stage III patients (p = 0.032; RR = 0.459; 95% confidence interval = 0.226–0.934) (data not shown).

Discussion

The purpose of our comprehensive combined CNA and gene expression analysis was to identify significant genes involved in distant metastasis of CRC. Comparing integrated CNA and gene expression data for patients with and without synchronous or metachronous distant metastasis, we found that the *NUCKS1* gene is significantly upregulated in patients with CRC with distant metastasis. Multivariate analysis of the results of immunohistochemical studies indicated that overexpression of the NUCKS1 protein is an independent and significant prognostic factor of CRC recurrence after curative surgery. This is the first study to demonstrate the clinical significance of the protein expression of a cancer-related gene identified using an integrated analysis.

The *NUCKS1* gene is located on chromosome 1q32.1. In a comprehensive meta-analysis comprising a total of 859 patients with CRC, Diep *et al.* found that the frequency of copy number gains at chromosome 1q significantly increased with Duke's stages, and that copy number gains at 1q are associated with established liver metastasis.[29] Their data are consistent with the present study with respect to the relationship between copy number gains and distant metastasis. Through integrated analysis of the high-resolution genome-wide copy number and matching expression data, we identified *NUCKS1* as an overexpressed gene with an amplified copy number on chromosome 1q. It has been reported that genes amplified in copy number are rarely overexpressed in colon cancers.[30] These rare copy

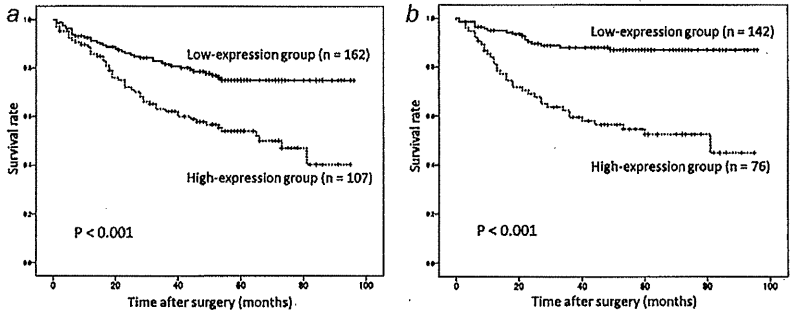

Figure 3. (*a*) Kaplan–Meier curves showing OS of 269 Stages I–IV CRC patients by NUCKS1 expression. (*b*) Kaplan–Meier curves showing RFS of 218 Stages I–III CRC patients by NUCKS1 expression.

Table 2. Relationship between clinicopathologic variables and NUCKS1 expression in patients with stage I-III colorectal cancer

Variables	NUCKS1 expression		p
	Low ($n = 142$)	High ($n = 76$)	
Age (Median), years	20–92 (74)	48–85 (65)	0.230
Gender			
Male	90	51	0.584
Female	52	25	
Histology			
Well	65	28	0.233
Moderate, poor and others	77	47	
Depth			
T1/T2	45	18	0.215
T3/T4	97	58	
Lymphatic invasion			
Negative	53	12	0.001
Positive	88	64	
Venous invasion			
Negative	27	5	0.013
Positive	114	71	
Lymph node metastasis			
Negative	97	35	0.001
Positive	45	41	
Carcinoembryonic antigen (ng/ml)			
<5	103	42	0.003
≥5	32	32	

number-amplified and overexpressed genes may play crucial roles in tumor progression. In this study, we found that elevated expression of NUCKS1 is related to distant metastasis and poor prognosis in patients with CRC, suggesting that the integration of expression and genomic profiling could be a useful approach for the discovery of cancer-related genes.

NUCKS1 has been characterized as a cell cycle-related protein,[23,24] and data suggest that it plays an important role in cell proliferation and cell progression by serving as a substrate for casein kinase 2 (CK-2) and the cyclin-dependent kinases (CDK) 1, CDK2, CDK4 and CDK6.[24,31–34] Although several reports have indicated that NUCKS1 is overexpressed in various cancer tissues and therefore may contribute to oncogenesis,[24–28] its precise role in cancer development remains unknown. This is the first study to demonstrate both the localization of NUCKS1 in CRC tissue and the relationship between NUCKS1 expression and prognosis in patients with CRC. We found that NUCKS1 staining tends to be stronger at the invasive tumor front than at the marginal site in CRC tissue. This result supports the hypothesis that overexpression of NUCKS1 at the invasive tumor front plays a critical role in the initiation of progression and metastasis of CRC. Further investigation is needed to confirm this hypothesis.

Table 3. Univariate and multivariate analysis of clinicopathologic factors affecting relapse-free survival in patients with stage I-III colorectal cancer

Variables	No. patients	Univariate analysis p	Multivariate analysis	
			Relative risk (95% confidence interval)	p
Age, years				
≤65	105	0.953		
>65	112			
Gender				
Male	141	0.159		
Female	77			
Histology				
Well	93	0.007		0.497
Moderate, poor and others	124			
Depth				
T1/T2	63	<0.001	0.275 (0.109–0.696)	0.006
T3/T4	155			
Lymphatic invasion				
Negative	65	<0.001		0.33
Positive	152			
Venous invasion				
Negative	32	0.015		0.617
Positive	185			
Lymph node metastasis				
Negative	132	<0.001	0.350 (0.192–0.638)	0.001
Positive	86			
Carcinoembryonic antigen (ng/ml)				
<5	145	<0.001		0.085
≥5	64			
NUCKS1 expression				
High	76	<0.001	0.286 (0.158–0.516)	<0.001
Low	142			

Surgery is still the most effective treatment for CRC. However, 40–50% of patients who undergo curative surgery ultimately suffer relapse.[35] Recently, various adjuvant chemotherapies have been shown to be associated with improved cure rates in patients with CRC who have undergone surgery.[36,37] It has also been shown that a 5-FU-based regimen with the addition of oxaliplatin, irinotecan or monoclonal antibodies can improve the outcome of cases of post-surgical recurrence.[38] However, even though these chemotherapies are effective, they are costly and carry the risk of severe adverse

effects.[39] It is important therefore to identify patients who are at high risk of recurrence for indication of adjuvant therapy or more aggressive treatment, as doing so will lead to improved prognosis and reduce both the cost of treatment and the risk of adverse effects. For this purpose reliable predictive biomarkers must be identified. Our study suggests that NUCKS1 might be a valuable biomarker of post-operative recurrence of CRC for use in deciding whether to use adjuvant chemotherapy or more intensive approaches in patients with CRC after surgery. It will be important to investigate the predictive value of NUCKS1 expression in Stage II and Stage III CRC patients enrolled in adjuvant chemotherapy clinical trials.

In conclusion, our results indicate that overexpression of NUCKS1 in CRC tissue is an independent prognostic factor for RFS in patients after curative surgery. NUCKS1 may therefore become a new biomarker for use in predicting the chances of recurrence after colorectal surgery. Blocking NUCKS1 may also represent a novel strategy for treating CRC.

Acknowledgements

Authors thank M. Itoda and Y. Takagi for excellent technical assistance.

References

1. Ricchi P, Zarrilli R, Di Palma A, et al. Nonsteroidal anti-inflammatory drugs in colorectal cancer: from prevention to therapy. *Br J Cancer* 2003;88:803–7.
2. Tsukuma H, Ajiki W, Oshima A. Cancer incidence in Japan. *Gan To Kagaku Ryoho* 2004;31:840–6.
3. Matsuda T, Marugame T, Kamo KI, et al. Cancer incidence and incidence rates in Japan in 2004: based on data from 14 population-based cancer Registries in the Monitoring of Cancer Incidence in Japan (MCIJ) Project. *Jpn J Clin Oncol* 2010; 40:1192–200.
4. Kobayashi H, Mochizuki H, Sugihara K, et al. Characteristics of recurrence and surveillance tools after curative resection for colorectal cancer: a multicenter study. *Surgery* 2007;141:67–75.
5. Weitz J, Koch M, Debus J, et al. Colorectal cancer. *Lancet* 2005;365:153–65.
6. Ross JS, Torres-Mora J, Wagle N, et al. Biomarker-based prediction of response to therapy for colorectal cancer: current perspective. *Am J Clin Pathol* 2010;134:478–90.
7. Shih W, Chetty R, Tsao MS. Expression profiling by microarrays in colorectal cancer (Review). *Oncol Rep* 2005;13:517–24.
8. Wang Y, Jatkoe T, Zhang Y, et al. Gene expression profiles and molecular markers to predict recurrence of Dukes' B colon cancer. *J Clin Oncol* 2004;22:1564–71.
9. Nannini M, Pantaleo MA, Maleddu A, et al. Gene expression profiling in colorectal cancer using microarray technologies: results and perspectives. *Cancer Treat Rev* 2009;35:201–9.
10. Nakao M, Kawauchi S, Furuya T, et al. Identification of DNA copy number aberrations associated with metastases of colorectal cancer using array CGH profiles. *Cancer Genet Cytogenet* 2009;188:70–6.
11. Kurashina K, Yamashita Y, Ueno T, et al. Chromosome copy number analysis in screening for prognosis-related genomic regions in colorectal carcinoma. *Cancer Sci* 2008;99:1835–40.
12. Yamamoto S, Midorikawa Y, Morikawa T, et al. Identification of chromosomal aberrations of metastatic potential in colorectal carcinoma. *Genes Chromosomes Cancer* 2010;49:487–96.
13. Aragane H, Sakakura C, Nakanishi M, et al. Chromosomal aberrations in colorectal cancers and liver metastases analyzed by comparative genomic hybridization. *Int J Cancer* 2001;94: 623–9.
14. Yau C, Holmes CC. CNV discovery using SNP genotyping arrays. *Cytogenet Genome Res* 2008; 123:307–12.
15. Tsafrir D, Bacolod M, Selvanayagam Z, et al. Relationship of gene expression and chromosomal abnormalities in colorectal cancer. *Cancer Res* 2006;66:2129–37.
16. Pollack JR, Sørlie T, Perou CM, et al. Microarray analysis reveals a major direct role of DNA copy number alteration in the transcriptional program of human breast tumors. *Proc Natl Acad Sci USA* 2002;99:12963–8.
17. Hyman E, Kauraniemi P, Hautaniemi S, et al. Impact of DNA amplification on gene expression patterns in breast cancer. *Cancer Res* 2002;62: 6240–5.
18. Phillips JL, Hayward SW, Wang Y, et al. The consequences of chromosomal aneuploidy on gene expression profiles in a cell line model for prostate carcinogenesis. *Cancer Res* 2001;61: 8143–9.
19. Ramakrishna M, Williams LH, Boyle SE, et al. Identification of candidate growth promoting genes in ovarian cancer through integrated copy number and expression analysis. *PLoS One* 2010; 5:e9983.
20. Cardoso J, Boer J, Morreau H, et al. Expression and genomic profiling of colorectal cancer. *Biochim Biophys Acta* 2007;1775:103–37.
21. Yoshida T, Kobayashi T, Itoda M, et al. Clinical omics analysis of colorectal cancer incorporating copy number aberrations and gene expression data. *Cancer Inform* 2010;9:147–61.
22. Nigro JM, Misra A, Zhang L, et al. Integrated array-comparative genomic hybridization and expression array profiles identify clinically relevant molecular subtypes of glioblastoma. *Cancer Res* 2005;65:1678–86.
23. Whitfield ML, Sherlock G, Saldanha AJ, et al. Identification of genes periodically expressed in the human cell cycle and their expression in tumors. *Mol Biol Cell* 2002;13:1977–2000.
24. Drosos Y, Kouloukoussa M, Østvold AC, et al. NUCKS overexpression in breast cancer. *Cancer Cell Int* 2009;9:19.
25. Sargent LM, Ensell MX, Ostvold AC, et al. Chromosomal changes in high- and low-invasive mouse lung adenocarcinoma cell strains derived from early passage mouse lung adenocarcinoma cell strains. *Toxicol Appl Pharmacol* 2008;233: 81–91.
26. Thompson HG, Harris JW, Wold BJ, et al. Identification and confirmation of a module of coexpressed genes. *Genome Res* 2002;12:1517–22.
27. Schaner ME, Ross DT, Ciaravino G, et al. Gene expression patterns in ovarian carcinomas. *Mol Biol Cell* 2003;14:4376–86.
28. Naylor TL, Greshock J, Wang Y, et al. High resolution genomic analysis of sporadic breast cancer using array-based comparative genomic hybridization. *Breast Cancer Res* 2005;7:R1186–R1198.
29. Diep CB, Kleivi K, Ribeiro FR, et al. The order of genetic events associated with colorectal cancer progression inferred from meta-analysis of copy number changes. *Genes Chromosomes Cancer* 2006;45:31–41.
30. Platzer P, Upender MB, Wilson K, et al. Silence of chromosomal amplifications in colon cancer. *Cancer Res* 2002;62: 1134–8.
31. Walaas SI, Ostvold AC, Laland SG. Phosphorylation of P1, a high mobility group-like protein, catalyzed by casein kinase II, protein kinase C, cyclic AMP-dependent protein kinase and calcium/calmodulin-dependent protein kinase II. *FEBS Lett* 1989;258:106–8.
32. Maelandsmo GM, Ostvold AC, Laland SG. Phosphorylation of the high-mobility-group-like protein P1 by casein kinase-2. *Eur J Biochem* 1989;184:529–34.
33. Ostvold AC, Norum JH, Mathiesen S, et al. Molecular cloning of a mammalian nuclear phosphoprotein NUCKS, which serves as a substrate for Cdk1 *in vivo*. *Eur J Biochem* 2001; 268:2430–40.
34. Meijer L, Ostvold AC, Walass SI, et al. High-mobility-group proteins P1, I and Y as substrates of the M-phase-specific p34cdc2/cyclincdc13 kinase. *Eur J Biochem* 1991;196: 557–67.
35. Obrand DI, Gordon PH. Incidence and patterns of recurrence following curative resection for colorectal carcinoma. *Dis Colon Rectum* 1997;40: 15–24.
36. André T, Boni C, Mounedji-Boudiaf L, et al. Oxaliplatin, fluorouracil, and leucovorin as adjuvant treatment for colon cancer. *N Engl J Med* 2004;350:2343–51.
37. Gray R, Barnwell J, McConkey C, et al. Adjuvant chemotherapy versus observation in patients with colorectal cancer: a randomised study. *Lancet* 2007;370:2020–9.
38. Wolpin BM, Mayer RJ. Systemic treatment of colorectal cancer. *Gastroenterology* 2008;134: 1296–310.
39. Aballéa S, Chancellor JV, Raikou M, et al. Cost-effectiveness analysis of oxaliplatin compared with 5-fluorouracil/leucovorin in adjuvant treatment of stage III colon cancer in the US. *Cancer* 2007;109:1082–9.